nature medicine

Article

https://doi.org/10.1038/s41591-026-04340-7

Trabectedin and low-dose irinotecan to target EWS::FLI1 in Ewing sarcoma: a phase 1/2 trial

Received: 1 November 2025

Accepted: 9 March 2026

Published online: 16 April 2026

Check for updates

A list of authors and their affiliations appears at the end of the paper

Ewing sarcoma (ES) is a bone and soft tissue sarcoma that is absolutely dependent on the EWS::FLI1 transcription factor for cell survival. No compound has been shown to reverse EWS::FLI1 activity in patients, and outcomes for relapsed patients remain poor. Trabectedin above a threshold concentration reverses the activity of EWS::FLI1 and is potentiated by low-dose irinotecan in vivo. This open-label phase 1/2 trial of trabectedin with irinotecan (SARC037) enrolled 37 relapsed/refractory patients with ES. The primary objectives were to determine the safety, tolerability, recommended phase 2 dose (RP2D; phase 1) and objective response rate (ORR; phase 2) of trabectedin administered as a 1-hour infusion in combination with low-dose irinotecan in patients with ES. The secondary objectives were to determine the progression-free survival (PFS), 6-month PFS, duration of response and ^{18}F-fluorothymidine positron emission tomography (^{18}F-FLT PET) avidity of ES tumors. The RP2D was trabectedin 1.0 mg m^{-2} over 1 hour (day 1) and irinotecan 25 mg m^{-2} (days 2 and 4) of a 21-day cycle. Toxicities were manageable with grade 3 or higher toxicities (>15%) of myelosuppression and alanine aminotransferase elevations at RP2D. The phase 2 ORR was 33% (39%, including RP2D phase 1 patients), and 6-month PFS was 48%. Transcriptional profiling demonstrated reversal of the EWS::FLI1 transcriptome in tumors from a subset of patients. Additional correlative objectives captured molecular profiling, circulating tumor DNA levels, pharmacokinetics and ^{18}F-FLT PET avidity. Here we provide the basis for further development of trabectedin/irinotecan for patients with ES by the international cooperative groups. ClinicalTrials.gov: NCT04067115.

Transcription factors are important but challenging drug targets in all human cancer types. ES is emblematic of tumors driven by oncogenic fusion transcription factors. Since the identification of the EWS::FLI1 transcription factor in the early 1990s, many studies have demonstrated a dependence of ES on EWS::FLI1 both in vitro and in vivo[1–6]. However, EWS::FLI1 is a challenging target because it exhibits a complicated interactome with numerous binding partners and a low-complexity transactivating domain that allows it to phase transition at enhancer elements[7,8]. In addition, the fusion protein uses several different mechanisms of action to both induce and repress transcription[7,9–14]. Nevertheless, because of the clear dependence of the tumor on this target, many groups have sought to identify compounds that inhibit EWS::FLI1 or its transcriptional program. A subset of these agents has been tested in patients with ES: cytarabine, trabectedin, YK-279, seclidemstat and mithramycin[15–23]. However, thus far, these approaches have been largely ineffective. Furthermore, outcomes for relapsed patients on ES

e-mail: grohar@med.umich.edu

clinical trials remain poor, with an ORR of only 10% in a meta-analysis of 827 patients enrolled on 62 trials between 2005 and 2018 (ref. 24).

Trabectedin is a natural product isolated from *Ecteinascidia turbinata* with a complicated and incompletely understood mechanism of action[25]. The drug binds to the DNA minor groove and generates DNA damage, poisons the DNA damage response, modulates the immune system and alters the activity of specific transcription factors in specific cell contexts[26–31]. Trabectedin induced an exceptional complete response in a patient with metastatic ES during a phase 1 study with a 3-hour infusion, and preclinical evidence suggested a heightened sensitivity of bone tumor cells[29,32,33]. We linked this response to inhibition of EWS::FLI1 and showed reversal of a highly specific NR0B1 luciferase reporter and reversal of a well-established list of EWS::FLI1 downstream targets[19]. A phase 2 trial that administered trabectedin as a 24-hour infusion did not show any activity, with only one of 10 evaluable patients with ES showing stable disease[22]. We further investigated trabectedin in ES cell lines and discovered that suppression of EWS::FLI1 requires a threshold concentration of drug to redistribute the fusion protein from the nucleoplasm into the nucleolus and trigger an epigenetic switch at EWS::FLI1 enhancers[34,35]. We correlated this mechanism with administration schedule and showed that the required threshold concentration of trabectedin was likely not achieved in the negative phase 2 (24-hour infusion) trial but may have been reached in the exceptional responder in the phase 1 study (3-hour infusion)[35]. Furthermore, we showed notable synergy with irinotecan where EWS::FLI1 suppression by trabectedin sensitized the cells to the DNA-damaging effects of irinotecan. Irinotecan, in turn, both amplified and sustained EWS::FLI1 suppression to demonstrate excellent activity in preclinical models[35,36]. Based on published pharmacokinetic data[37], we hypothesized in the present study that administration of trabectedin as a 1-hour infusion would likely exceed the threshold concentration to reverse EWS::FLI1 activity and realize the described synergy with irinotecan to drive responses in patients with ES.

We thus developed SARC037, an open-label phase 1/2 trial of trabectedin administered as a 1-hour infusion in combination with low-dose irinotecan in patients with ES. The primary objectives were to determine the safety, tolerability and recommended dose of trabectedin and low-dose irinotecan (phase 1 (Ph1)) and to determine the antitumor activity as measured by the tumor ORR assessed by Response Evaluation Criteria in Solid Tumors version 1.1 (RECIST 1.1) (phase 2 (Ph2)). Exploratory objectives included determining the effect of treatment on EWS::FLI1 transcriptional networks and if ^{18}F-FLT PET suppression and/or trabectedin serum maximal concentration (C_{max}) or area under the curve (AUC) exposure correlates with EWS::FLI1 suppression. Additional exploratory objectives were to determine if tumor mutational profiling, change in circulating tumor DNA (ctDNA) burden or EWS::FLI1 fusion type were associated with treatment response.

Results

Patient characteristics

A total of 37 patients with relapsed/refractory ES, age ≥ 10 years (Ph1) or ≥6 years (Ph2), with a confirmed EWS::FLI1 translocation, adequate performance status (Eastern Cooperative Oncology Group (ECOG) 0–2) and evaluable (Ph1) or measurable (Ph2) disease were enrolled between 5 January 2021 and 31 December 2023. Nineteen patients enrolled in Ph1 and 18 patients in Ph2, all with participation in correlative studies (Fig. 1a). Two patients were replaced during the dose-escalation phase because they were not evaluable for dose-limiting toxicities (DLTs) due to rapid progression or comorbidities (Fig. 1a). The patient demographics (Table 1) reflected those of the disease, with most being white (Ph1 = 89%, Ph2 = 67%) and male (Ph1 = 74%, Ph2 = 56%). All patients had advanced, relapsed or refractory disease and, in both phases, had a median of four prior lines of therapy. Most patients had previously received irinotecan (Ph1 = 63%, Ph2 = 67%), and most had metastatic disease, with the most common site being lung (Ph1 = 100%, Ph2 = 72%).

Safety, tolerability and RP2D

Four dose levels (DLs) were evaluated during Ph1, and the RP2D was DL2: trabectedin 1.0 mg m^{-2} given as a 1-hour infusion on day 1 and irinotecan 25 mg m^{-2} days 2 and 4 included grade 4 neutropenia (DL3), grade 3 vascular access complication (thrombosis; DL3), grade 3 infection (DL4) and grade 3 fatigue (DL4) (Table 2). There were two grade 5 events in the Ph1 portion of the study. The first patient had an unconfirmed partial response after four cycles and had recovered from toxicities from the prior cycle. The patient developed sudden-onset respiratory distress during the time of the COVID pandemic and transitioned to home hospice, declining a medical evaluation. The second patient began therapy 3 days after chest tube placement for progressive effusions and decompensated on day 5 with hypotension, tachycardia, fever and hypoxia and was determined to have sepsis, although no infectious source was identified. There were no grade 5 events in Ph2.

The combination was well tolerated in most patients in Ph2, with the most common grade 3/4 toxicities (>15% of patients) being myelosuppression: grade 3 anemia (26%); grade 3/4 neutropenia (60%); grade 3/4 lymphopenia (26%); and thrombocytopenia (52%) (Extended Data Table 1). Only three patients (13%) demonstrated grade 4 alanine aminotransferase elevations, and only one patient (4%) experienced grade 3 diarrhea. Furthermore, only one patient (4%) experienced grade 3 nausea. Two patients discontinued treatment due to toxicity in Ph2, one due to laboratory abnormalities that did not normalize within the protocol-defined window and one due to patient preference secondary to grade 3 fatigue.

Tumor response

A secondary objective of the Ph1 portion and the primary objective of the Ph2 portion of the study was to determine the ORR (per RECIST 1.1). Trabectedin activity was dose dependent in Ph1, with zero of three responders at DL1 and three confirmed partial responses in five patients (60%) at DL2 (Fig. 1b–d). A total of four patients in Ph1 had confirmed partial responses. An additional four patients had more than 20% reduction in tumor size lasting at least 100 days that did not meet criteria for a confirmed partial response. Increased irinotecan dose did not appear to improve activity, as patients enrolled on DL2 and DL4 both received 1.0 mg m^{-2} trabectedin, but increasing irinotecan from 25 mg m^{-2} (DL2; $n = 5$; ORR = 60%) to 30 mg m^{-2} (DL4; $n = 6$; ORR = 0%) was associated with less activity, an observation that trended toward significance ($P = 0.061$) (Fig. 1d). Activity was sustained, with an overall 6-month PFS of 32% (95% confidence interval = 16.2–61.2%) across all DLs (Extended Data Fig. 1).

The Ph2 portion of the study met the predetermined success criterion with confirmed partial responses in six of 18 patients (33%), with an additional three patients achieving stable disease (Fig. 2a). Overall, confirmed objective responses occurred in nine of 23 patients (39%) treated at the RP2D ($n = 5$, Ph1; $n = 18$, Ph2) (Figs. 1b and 2a). Notably, in responding patients, the response was sustained, and all Ph2 responders were on study for at least 10.5 months (Fig. 2b). Response appeared to be independent of the number of prior lines of therapy, with two of the best responders having received five prior treatment regimens (see asterisk in Fig. 2b). Overall, the 6-month PFS was 48% in Ph2.

Identification of biomarkers of objective response

The Ph2 portion of the study showed a binary response pattern, with either a relatively rapid and durable response for ≥10–12 months or early progression (Fig. 2b). Clinical factors did not appear to distinguish responders from non-responders, as the number of prior lines of therapy ($P = 0.7$), tumor burden (of target lesions ($P = 0.5$)), translocation type ($P = 0.9$) and prior irinotecan ($P > 0.9$) were not significantly different between the groups (Extended Data Table 2a).

By contrast, the patients with no detectable ctDNA on day 8 ($n = 9$) in both Ph1 and Ph2 had significantly longer PFS than those with detectable ctDNA ($n = 28$; $P = 0.0078$) (Fig. 2c). This was not simply a function

https://doi.org/10.1038/s41591-026-04340-7

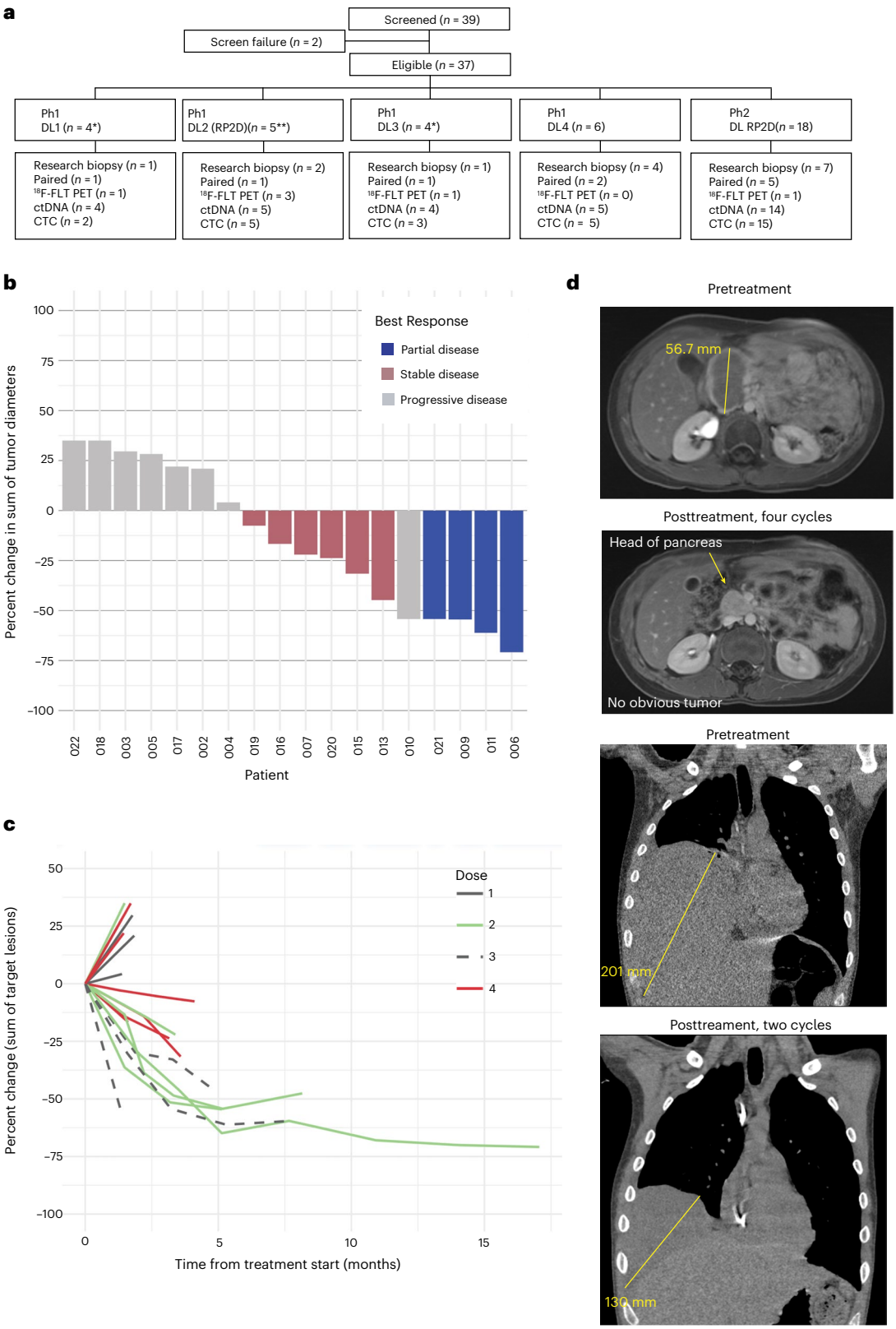

Fig. 1 | Ph1 enrollments and patient responses. a, CONSORT diagram showing enrollment characteristics and correlative biology specimen acquisition. Research biopsy numbers include only patients enrolled on the study consented to any biopsy (eight in Ph1, seven in Ph2). Paired biopsies are before and after trabectedin administration but prior to irinotecan. Circulating tumor DNA (ctDNA) and circulating tumor cell (CTC) samples required a pretreatment and at least one other timepoint to be included. A total of six patients had ^{18}F-FLT PET imaging, but only four were paired before and after trabectedin administration. (*) Patients replaced for rapid progression, making them unevaluable for dose limiting toxicity (DLT). (**) Includes two patients enrolled in the expansion cohort. **b**, Target lesion best response per RECIST 1.1 by patient. Colors capture confirmed partial response (blue), stable disease (red) or progressive disease (gray). **c**, Spaghetti plot demonstrating patient response as a function of dose level (DL). Note the response in DL2 ($n = 5$, green = 1.0 mg m^{-2} T (trabectedin) (day 1) and 25 mg m^{-2} I (irinotecan) (days 2 and 4)) versus DL4 ($n = 6$, red = 1.0 mg m^{-2} T (day 1) and 30 mg m^{-2} I (days 2 and 4)). **d**, Response of two patients enrolled at DL2.

https://doi.org/10.1038/s41591-026-04340-7

Table 1 | Patient demographics

Characteristic	Ph1 (*n*=19)	Ph2 (*n*=18)
	Number (%)	Number (%)
Age at enrollment		
Median (range)	19 (10–59)	21 (9–43)
Age ≥18 years at enrollment		
	12 (63%)	12 (67%)
Age ≥18 years at diagnosis		
	7 (37%)	9 (50%)
Sex		
Female	5 (26%)	8 (44%)
Male	14 (74%)	10 (56%)
Race		
White	17 (89%)	12 (67%)
Asian	2 (11%)	1 (5%)
Black or African heritage		1 (5%)
Other		4 (22%)
Ethnicity		
Hispanic/Latino	2 (11%)	4 (22%)
Not Hispanic/Latino	17 (89%)	14 (78%)
Performance status		
ECOG 0/Lansky 90–100	13 (69%)	9 (50%)
ECOG 1/Lansky 70–80	3 (16%)	8 (44%)
ECOG 2/Lansky 50–60	3 (16%)	1 (6%)
Prior therapy		
Median prior lines of systemic therapy (range)	4 (2–9)	4 (1–7)
Number of prior lines of therapy		
1–2	2 (11%)	4 (22%)
3–4	9 (47%)	9 (50%)
≥5	8 (42%)	5 (28%)
Prior irinotecan	12 (63%)	12 (67%)
Prior surgical local control	17 (89%)	17 (94%)
Prior radiation	16 (84%)	16 (89%)
Primary site		
Extremity	8 (42%)	4 (22%)
Pelvis	3 (16%)	5 (28%)
Chest wall	2 (11%)	4 (22%)
Other	6 (32%)	5 (28%)
Primary tumor origin		
Bone	16 (84%)	13 (72%)
Soft tissue/extraskeletal	3 (16%)	5 (28%)
Sites of metastases at time of enrollment		
Lung/pleural	19 (100%)	13 (72%)
Bone	6 (32%)	7 (39%)
Visceral	3 (16%)	1 (6%)
Other	8 (42%)	6 (33%)

of tumor burden or ctDNA level at baseline as there was no difference in outcomes for patients who had detectable ctDNA versus those who did not at pretreatment baseline (Extended Data Fig. 2). Furthermore, if the patients with negative ctDNA at baseline are removed from the ctDNA analysis at day 8, the stratification remains highly significant ($P < 0.016$) (Extended Data Fig. 3). To identify molecular factors associated with response, all patients in Ph1/Ph2 had tumor mutation profiling performed (Ph2, Fig. 2d; Ph1, Extended Data Fig. 4). The numbers were too small to demonstrate a mutation profile associated with patient response. However, mutations in *CDKN2A*, *SMARCA4* and Notch were enriched in responders—a pattern that was significant for mutations in Notch ($P = 0.047$; Extended Data Table 2b). By contrast, gains in chromosome 8, mutations in *EZH2* and mutations in *STAG2* were enriched in non-responders (Extended Data Table 2b).

An important observation was a higher-than-expected frequency of non-type I and type II EWS::FLI1 fusions in this heavily pretreated, treatment-refractory population that showed a statistically significant association with the number of prior lines of therapy ($P = 0.036$) but not with response to trabectedin/irinotecan (Extended Data Table 3). Notably, alternative exon usage was found primarily in DNA-based translocation testing assay results.

EWS::FLI1 transcriptional profiling

The premise of the study was that a 1-hour infusion of trabectedin would achieve serum levels sufficient to inhibit EWS::FLI1, the driver oncogene. Therefore, to evaluate the impact of trabectedin on EWS::FLI1 activity, a subset of patients had research biopsies for transcriptional profiling before and after trabectedin and prior to irinotecan administration. A total of 15 patients (eight Ph1 and seven Ph2) consented to and underwent biopsies. Of the 15, eight had pretreatment and posttreatment biopsy pairs amenable to RNA sequencing (one had a biopsy at progression only; five were pretreatment or posttreatment only; and RNA purification was inadequate in one). Three of the eight patients (013, 038 and 011) showed clear reversal of the 'Lessnick list'[38] of EWS::FLI1 target genes (Fig. 3a and Extended Data Fig. 5). As examples, patient 013 showed clear reversal of the transcriptome and a RECIST-confirmed partial response, whereas patient 016 did not show reversal and had limited disease stabilization (Fig. 3a). This patient came off study due to unacceptable toxicity that limited the evaluation of response.

To validate the bulk RNA sequencing results using a complementary platform, we used spatial transcriptomics to demonstrate suppression of the EWS::FLI1 transcriptome in patient 013 (Fig. 3b,c). Tumor was distinguished from normal using a *k*-means approach ($n = 2$). We observed a decrease in the log-normalized unique molecular identifier (UMI) counts from 1.94 to 1.37 for a 10-gene composite signature of well-established EWS::FLI1-driven GGAA microsatellite genes: *NROB1*, *IL1RAP*, *EZH2*, *CAV1*, *AKAP7*, *CACNB2*, *RCOR1*, *FCGRT*, *FEZF1* and *FOCAD*[12,39–42]. Interestingly, the suppression of EWS::FLI1 by trabectedin was not uniform throughout the tumor, yielding a small population of cells with persistently high activity best demonstrated in uniform manifold approximation and projection (UMAP) plots of *NROB1* expression (Fig. 3d), the 10-gene GGAA microsatellite signature (Fig. 3e) or the Lessnick list[38] of EWS::FLI1 induced targets (Fig. 3f).

To increase the statistical rigor of the analysis, we pooled the data from spatial transcriptomics from five pretreatment and posttreatment pairs (patients 013, 015, 029, 032 and 033) and demonstrated highly significant reversal of expression of the Lessnick list[38] of EWS::FLI1 induced ($P = 0$) and repressed ($P = 5 \times 10^{-222}$) targets (Fig. 3g). To increase specificity, we filtered the 503-gene Lessnick induced target list to include only 175 targets that had EWS::FLI1 bound to GGAA microsatellites within 250 kbp, a distance defined in the ES cell lines atlas[43]. Individual tumors showed highly significant suppression of this 175-gene signature (Fig. 3h). The number of patients was too small to associate patient response and EWS::FLI1 suppression. However, trabectedin clearly reversed expression of the EWS::FLI1 transcriptome in patients using two different platforms and three independent EWS::FLI1 signatures.

^{18}F-FLT PET imaging

We assessed the utility of ^{18}F-FLT PET as a pharmacodynamic marker of EWS::FLI1 activity. ^{18}F-FLT is a radiolabeled thymidine that is used as an imaging marker of cancer cell proliferation[44]. We demonstrated

https://doi.org/10.1038/s41591-026-04340-7

Table 2 | Ph1 grade 3/4 treatment-emergent adverse events by DL

Adverse event	DL1 Tr 0.8 mg m^{-2} Ir 25 mg m^{-2} per dose (*n*=4)		DL2/ expansion Tr 1.0 mg m^{-2} Ir 25 mg m^{-2} per dose (*n*=5)		DL3 Tr 1.1 mg m^{-2} Ir 25 mg m^{-2} per dose (*n*=4)		DL4 Tr 1.0 mg m^{-2} Ir 30 mg m^{-2} per dose (*n*=6)	
CTCAE grade	3	4	3	4	3	4	3	4
Blood disorders								
Anemia	-	-	2 (40)	-	2 (50)	1 (25)	4 (67)	-
Febrile neutropenia	-	-	2 (40)	-	3 (75)	-	3 (50)	-
Leukopenia	-	-	2 (40)	1 (20)	-	2 (50)	1 (17)	-
Lymphopenia	-	-	1 (20)	1 (20)	2 (50)	-	1 (17)	2 (33)
Neutropenia	2 (50)	-	1 (20)	3 (60)	-	1 (25)*	-	4 (67)
Thrombocytopenia	1 (25)	-	-	3 (60)	-	2 (50)	-	1 (17)
Gastrointestinal disorders								
Diarrhea	-	-	1 (20)	-	1 (25)	-	-	-
Mucositis	-	-	1 (20)	-	-	-	-	-
Nausea/vomiting	-	-	-	-	1 (25)	-	-	-
General disorders								
Fatigue/malaise	-	-	1 (20)	-	-	-	1 (17)	-
Anaphylaxis	-	-	1 (20)	-	-	-	-	-
Infections								
Skin infection	-	-	-	-	-	-	1 (17)	-
Investigations								
ALT/AST elevation	1 (25)	1 (25)	3 (60)	-	2 (50)	-	3 (50)	-
GGT elevation	1 (25)	-	-	-	-	-	1 (17)	-
CPK elevation	-	-	2 (40)	-	-	-	-	1 (17)
Metabolism and nutrition disorders								
Dehydration	-	-	1 (20)	-	1 (25)	-	-	-
Hyperphosphatemia	-	-	1 (20)	-	-	-	-	-
Hypokalemia	-	-	-	-	-	-	-	-
Musculoskeletal and connective tissue disorders								
Pain	1 (25)	-	-	-	-	-	1 (17)	-
Rhabdomyolysis	-	-	-	-	-	-	1 (17)	-
Respiratory disorders								
Hypoxia	-	-	-	-	1 (25)	-	1 (17)	-
Vascular disorders								
Hypotension	-	-	-	-	-	1 (25)	-	-

ALT, alanine aminotransferase; AST, aspartate aminotransferase; CPK, creatine phosphokinase; GGT, gamma-glutamyl transferase; Ir, irinotecan dose administered intravenously on days 2 and 4; Tr, trabectedin dose administered intravenously over 1 hour on day 1. Asterisk (*) indicates DLTs.

in preclinical models that the proteins responsible for ^{18}F-FLT activity in ES cells (ENT1/ENT2/TK1) are downstream targets of EWS::FLI1 (ref. 45). ES xenografts were, therefore, highly ^{18}F-FLT PET avid. Reversal of EWS::FLI1 activity using an alternative EWS::FLI1 targeted agent, mithramycin[20], blocked ^{18}F-FLT signal in the xenograft tumor[45].

Six patients had ^{18}F-FLT scans, including four with paired imaging before and after trabectedin treatment. Two patients had ^{18}F-FLT PET imaging later during therapy. Consistent with the preclinical report, ES tumors in patients on this trial showed notable ^{18}F-FLT PET activity analogous to ^{18}F-fluorodeoxyglucose (FDG) PET but with a notably different distribution consisting of high marrow signal but limited signal in the brain and heart (Fig. 4a and Extended Data Fig. 6). Similar to ^{18}F-FDG PET, the scan proved useful to track tumor burden and to delineate active tumor from residual scar tissue (Fig. 4b and Extended Data Fig. 6). Furthermore, in one patient, three of four lesions on day 403 showed complete resolution, while the site that retained ^{18}F-FLT PET activity was the site of recurrence (Fig. 4c). Unfortunately, although some tumors showed limited suppression of ^{18}F-FLT PET signal with trabectedin treatment, overall, the suppression was minimal.

Clinical pharmacology

We hypothesized that EWS::FLI1 reversal could be achieved if a threshold concentration of trabectedin is exceeded by using a 1-hour infusion. Pharmacokinetic profiling was performed in Ph1 (Methods). The analysis of plasma pharmacokinetics was stratified by DL and incorporated data from 22 patients, including all patients enrolled in the Ph1 cohort (Extended Data Fig. 7).

Patients were given varying doses of trabectedin ranging from 0.8 mg m^{-2} to 1.1 mg m^{-2} (1.1–2.4 mg). End-of-infusion samples, typically representative of C_{max} values for intravenous-infused drugs, were not available for patients receiving serial sample collection in this cohort and were, thus, simulated using a population pharmacokinetic

https://doi.org/10.1038/s41591-026-04340-7

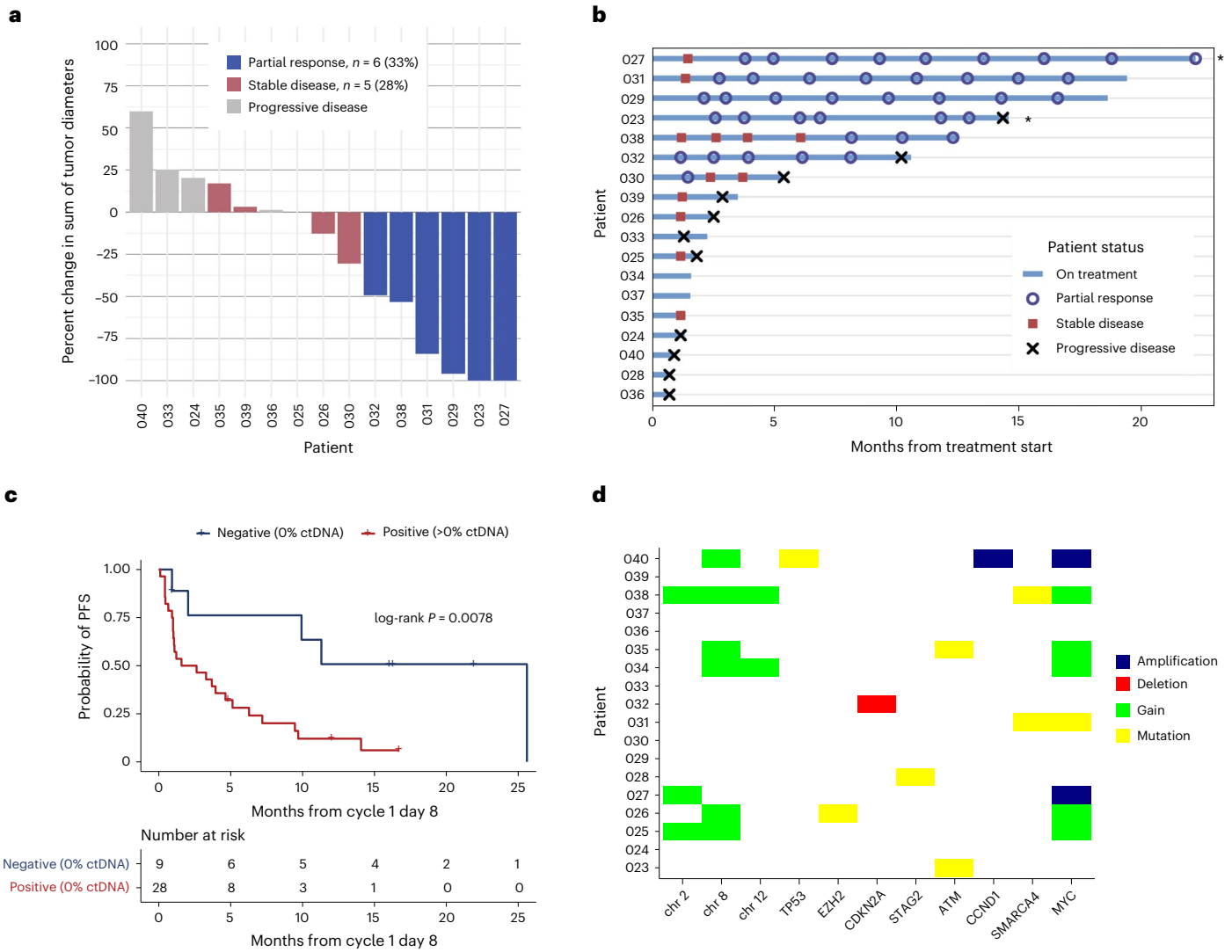

Fig. 2 | Ph2 response and pooled response predictors. a, Target lesion response per RECIST 1.1 as a function of Ph2 patient. Three patients are excluded due to rapid progression and baseline measurements only. **b**, Swimmer plot showing duration of response in months as a function of patient. Asterisk (*) indicates patient enrolled as sixth-line therapy. **c**, Kaplan–Meier survival curves featuring survival as a function of time in months for all patients in Ph1 and Ph2 stratified by non-detectable (blue) and detectable (red) ctDNA on day 8 ($P = 0.0078$). Analysis was performed using the log-rank test ($\chi^2 = 7.1$, 1 df), with a hazard ratio of 3.96 (95% confidence interval: 1.34–11.7). **d**, Oncoplot showing somatic mutations in Ph2 patient population as a function of patient identification number. df, degree of freedom.

(popPK) model previously established in both adult and adolescent patient cohorts[46,47]. Mean simulated C_{max} estimates by DL (0.8 mg m^{-2}: 16.24 ± 2.13 ng ml^{-1}; 1.0 mg m^{-2}: 25.17 ± 6.20 ng ml^{-1}; 1.1 mg m^{-2}: 30.86 ± 3.03 ng ml^{-1}) were more than 20% greater than previously published values for patients receiving a 1-hour infusion (0.8 mg m^{-2}: 13 ± 6.9 ng ml^{-1}; 1.0 mg m^{-2}: 17 ± 5.2 ng ml^{-1}; 1.1 mg m^{-2}: 18 ± 4.5 ng ml^{-1})[48]. Similarly, mean trabectedin exposures (measured via area under the curve (AUC)) (0.8 mg m^{-2}: 44.80 ± 17.78 h × ng ml^{-1}; 1.0 mg m^{-2}: 63.57 ± 21.94 h × ng ml^{-1}; 1.1 mg m^{-2}: 130.4 ± 70.49 h × ng ml^{-1}) were approximately two times greater than previously published values (0.8 mg m^{-2}: 23 ± 7.5 h × ng ml^{-1}; 1.0 mg m^{-2}: 36 ± 6.4 h × ng ml^{-1}; 1.1 mg m^{-2}: 52 ± 16 h × ng ml^{-1})[48]. Dose-normalized values for C_{max} and AUC (C_{max}/dose and AUC/dose, respectively) were similar across all DLs.

Discussion

In this report, we show, to our knowledge for the first time, reversal of the EWS::FLI1 transcriptome in patients with the drug trabectedin. Although the dependence of ES on EWS::FLI1 has been known for over 25 years, no drug has achieved therapeutic suppression of this enigmatic drug target. In the present study, we sought to realize our preclinical observation that trabectedin reverses the EWS::FLI1 transcriptome by a mechanism that requires a threshold concentration of drug.

Historical pharmacokinetic data suggested that this threshold would likely be surpassed if the drug was given as a 1-hour infusion versus the traditional 24-hour infusion schedule. Indeed, we showed convincing suppression of the EWS::FLI1 transcriptome in patient samples from both Ph1 and Ph2 using two separate platforms: bulk RNA sequencing and spatial transcriptomics. This translated into a positive Ph2 study in a heavily pretreated patient population with an acceptable toxicity profile and a 39% ORR in patients treated at the RP2D in Ph1/Ph2. This response rate compares favorably to the 10% ORR of 827 patients with ES treated on 62 studies between 2005 and 2018 or the more recently reported 10% (regorafenib) or 26% (cabozantinib) ORR for tyrosine kinase inhibitors[24,49,50]. Our overall 6-month PFS rate of 48% in Ph2 likewise compares favorably to rates of 12% in prior Children's Oncology Group Ph2 trials and 26% for a Ph2 trial of regorafenib, which has now advanced to frontline testing in this disease[51,52]. Furthermore,

https://doi.org/10.1038/s41591-026-04340-7

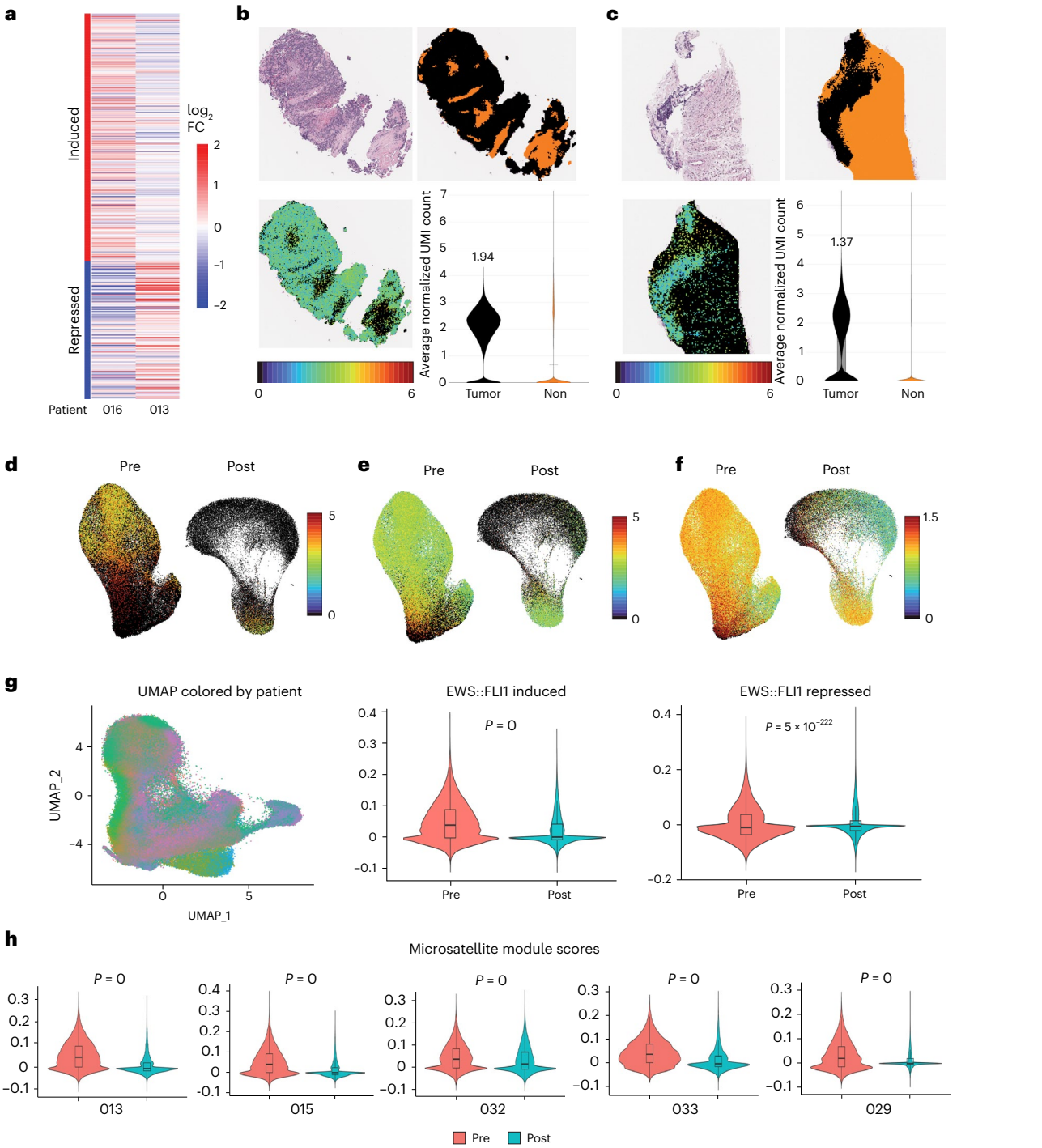

Fig. 3 | Trabectedin suppresses the EWS::FLI1 transcriptional program. **a**, Heatmap showing log_2FC expression of the 'Lessnick list' of EWS::FLI1 induced (top) and repressed (bottom) targets of patient 013 (right) and patient 016 (left). Spatial transcriptomics using *k*-means ($n = 2$) to distinguish tumor (black) from normal (orange), quantitated as average log-normalized UMI count per cell of 10-gene microsatellite signature represented as a heatmap (scale below image). Before (**b**) or after (**c**) treatment with trabectedin and prior to irinotecan administration. UMAP plot showing penetrance of suppression of NR0B1 (log-normalized expression) (**d**) or 10-gene microsatellite list (**e**) or Lessnick list of induced targets quantitated as log-normalized average UMI count per cell with heatmap adjacent depicting scale (**f**). **g**, UMAP composite view of five tumors before treatment and after treatment demonstrating statistically significant suppression of EWS::FLI1 from a median of 0.0393 (IQR 0.09) to 0 (IQR 0.049) ($P = 0$) for induced targets and induction of EWS::FLI1 repressed targets from −0.0076 (IQR 0.073) to −0.003 (IQR 0.036) ($P = 5 \times 10^{-222}$). **h**, Impact of trabectedin on expression of the EWS::FLI1 microsatellite-bound induced target genes ($n = 175$; Methods) in five separate sample pairs showing suppression from patient 013 = (0.048 (IQR 0.096) to −0.0035 (IQR 0.036)), patient 015 = (0.040 (IQR 0.092) to −0.0001 (IQR 0.033)), patient 032 = (0.037 (IQR 0.085) to −0.0015 (IQR 0.076)), patient 033 = (0.036 (IQR 0.077) to −0.003 (IQR 0.044)) and patient 029 = (0.019 (IQR 0.082) to −0.0009 (IQR 0.023)). The data are presented as violin plots where the width represents the kernel density, the line indicates median, the box indicates the IQR range (25th to 75th percentiles) and the whiskers indicate 1.5× IQR. *P* values were determined by Wilcoxon rank-sum test with multiple testing correction using the Benjamini–Hochberg method. FC, fold change; IQR, interquartile range.

https://doi.org/10.1038/s41591-026-04340-7

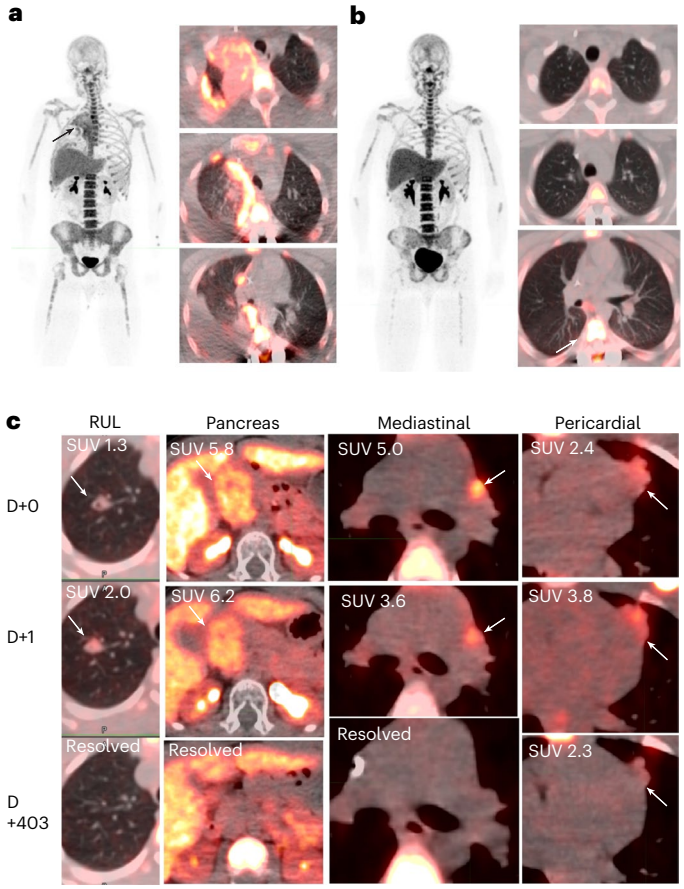

Fig. 4 | ^{18}F-FLT is a biomarker of tumor response and recurrence. ^{18}F-FLT PET scan demonstrating high tumor burden at onset of therapy (**a**) with tumor response and one persistent lesion (white arrow) in patient 023 after four cycles of trabectedin/irinotecan (**b**). **c**, ^{18}F-FLT shows variable signal suppression in patient 006 with trabectedin exposure and near-complete resolution of tumor by day 403 with one persistent lesion that proved to be the site of recurrence. D, day; RUL, right upper lobe; SUV, standard uptake value.

consistent with poisoning the driver oncogene of the tumor, many responses were sustained, despite treating a patient population with a median of four prior lines of therapy.

This study clearly shows that the genetic context of a specific tumor can be a critical determinant of drug synergy, optimal dosing and schedule of administration. We show that less trabectedin (1.0 mg m^{-2}) is more effective when given over 1 hour compared to 1.5 mg m^{-2} over 24 hours in previous ES trials. Notably, the 24-hour infusion schedule was used in the previous study because trabectedin was more active with this schedule in other sarcomas (not ES)[53]. That study, plus the exceptional response of a Ph1 patient with ES that occurred with a 3-hour infusion schedule, drove our preclinical studies that led to the observations supporting the 1-hour infusion schedule used in the present study[34,35]. Furthermore, a previous study showed similar exposure between 1-hour and 3-hour infusions of trabectedin, suggesting that a shorter infusion time and higher C_{max} concentrations may be associated with increased clinical efficacy in ES[48].

Evaluation of C_{max} concentrations for this cohort was a limitation of this study. Trabectedin has a rapid distribution phase after reaching C_{max}, resulting in a >10-fold reduction in plasma concentration within 0.5–2 hours after end of infusion[46–48]. Although a popPK model was used to simulate C_{max}, the model-predicted concentrations should be considered inferior to appropriately timed quantitated plasma concentrations. End-of-infusion samples were collected only in a small subset of Ph2 patients, and even small variations in collection times could significantly impact values obtained, necessitating this accepted modeling approach. Additionally, the AUC timepoints were different than previous reports, likely accounting for the approximately two-fold increase compared to previously published values[48]. Future pharmacokinetic studies will be required to better understand the relationship among C_{max}, AUC and clinical efficacy. Nevertheless, the C_{max} values reported in this study are consistent with previous publications and the goal levels that led to this study design. These concentrations would be expected to show an effect on EWS::FLI1 in our preclinical models.

Synergy is also context dependent. Most of the patients who responded on this study had previously experienced disease progression on irinotecan-containing regimens that included 200–250 mg m^{-2} total dose per cycle. Here, we use only 50 mg m^{-2} and, as a result, saw only one patient with grade 3 or higher diarrhea in Ph2. Escalation of irinotecan in the present study led to both more toxicity and, somewhat surprisingly, less activity in the Ph1 portion of the study. DL4 (1.0 mg m^{-2} trabectedin and 30 mg m^{-2} irinotecan; $n = 6$) had zero responders in Ph1, whereas DL2 and expansion (1.0 mg m^{-2} trabectedin and 25 mg m^{-2} irinotecan; $n = 5$) had three confirmed partial responses ($P = 0.061$). By linking the synergy to the driver oncogene of the tumor, EWS::FLI1, we were able to have more activity with less drug and, hence, less toxicity. We, therefore, advanced DL2 with lower-dose irinotecan into the Ph2 portion of the trial.

In patients who responded, the response was sustained, and all patients who responded in Ph2 remained on study for at least 10.5 months. The responses occurred almost immediately and often showed a sustained and steady decrease in tumor size instead of a dramatic decrease in tumor burden as seen with DNA-damaging agents. Because every patient had confirmation of the presence of the EWS::FLI1 fusion protein, it is not clear why some patients responded while others did not. Clinical factors such as tumor burden at the time of therapy, number of prior lines of therapy, exposure to prior irinotecan or disease burden did not distinguish responders from non-responders. There did appear to be a trend toward specific molecular alterations such as mutation in *CDKN2A*, *SMARCA4* and Notch favoring responders, whereas gain in chromosome 8 or mutations in *EZH2* and *STAG2* were more frequently detected in non-responders. Patient numbers were ultimately too small to consider any of these as potential enrichment biomarkers for future trials. However, ctDNA changes as early as day 8 did identify patients most likely to have an extended PFS independent of starting ctDNA burden. This is an exciting observation that will be an important biomarker for future studies with this agent and combination.

Notably, this study also provides important insight into the therapeutic targeting of transcription factors and EWS::FLI1 in particular. In our hands, bulk RNA sequencing did not prove to be an adequate assay to show suppression. Even though the samples were image-guided biopsies, they proved to be highly heterogeneous. This led to inconsistent evidence of suppression of EWS::FLI1 using bulk RNA sequencing. However, spatial transcriptomics proved to be a powerful assay to capture EWS::FLI1 suppression. Although our *k*-means approach did separate tumor from normal easily in some patients, it did not extend to all samples, which required more extensive analysis to separate tumor from normal. We, therefore, pooled all the samples to confirm EWS::FLI1 suppression. However, it is notable that it is not known how the EWS::FLI1 transcriptome changes immediately after exposure to conventional chemotherapy, as these studies have not been done. A critical question will be to understand how trabectedin modulation of the 'Lessnick signature' differs from the response to conventional chemotherapy and how both can be improved. For trabectedin, a deeper understanding of the molecular mechanisms responsible for EWS::FLI1 suppression is needed. For conventional therapies, this will require an increased willingness to partner with patients to obtain more pretreatment and posttreatment tumor samples to better understand the transcriptional dynamics of the tumor. Nevertheless, specimens collected in this biology-forward trial will be used to propose several

biomarkers of response that can be tested for predictive power in future studies.

Finally, ^{18}F-FLT did not prove to be a biomarker of EWS::FLI1 suppression. There was minor suppression in some patients accompanied by a non-specific change in marrow signal. In hindsight, the tracer was developed using an alternative EWS::FLI1 targeted agent, mithramycin[20], or by small interfering RNA (siRNA) silencing of EWS::FLI1. Although a follow-up preclinical study did show suppression of ^{18}F-FLT PET signal after trabectedin exposure[35], it is not clear why that did not translate to this clinical study. In the future, ^{18}F-FLT PET may be an effective biomarker for mithramycin, its second-generation analog, AIT-102 (ref. 54), or other future EWS::FLI1 modulators. However, this study showed that ES is highly ^{18}F-FLT PET avid. The tracer showed similar sensitivity as ^{18}F-FDG PET but a different distribution of background that might make it useful in areas where ^{18}F-FDG PET is less useful, such as the brain. Furthermore, the ^{18}F-FLT tracer avidity proved to be an early predictor of recurrence, remaining avid in residual tissue with active tumor.

In summary, the combination of trabectedin and irinotecan is tolerated and active in ES and warrants further investigation. The combination is associated with EWS::FLI1 suppression and causes marked and sustained tumor regressions in a subset of heavily pretreated patients with ES. The identification of patients who are most likely to respond is a critical area of ongoing research. Nevertheless, this is a promising new drug combination for ES and is being further developed in the cooperative groups in Europe (EuroEwing Consortium) and the United States (Children's Oncology Group).

Online content

Any methods, additional references, Nature Portfolio reporting summaries, source data, extended data, supplementary information, acknowledgements, peer review information; details of author contributions and competing interests; and statements of data and code availability are available at https://doi.org/10.1038/s41591-026-04340-7.

References

1. Delattre, O. et al. Gene fusion with an *ETS*DNA-binding domain caused by chromosome translocation in human tumours. *Nature* **359**, 162–165 (1992).
2. Delattre, O. et al. The Ewing family of tumors—a subgroup of small-round-cell tumors defined by specific chimeric transcripts. *N. Engl. J. Med.* **331**, 294–299 (1994).
3. Kovar, H. et al. EWS/FLI-1 antagonists induce growth inhibition of Ewing tumor cells in vitro. *Cell Growth Differ.* **7**, 429–437 (1996).
4. Dohjima, T., Lee, N. S., Li, H., Ohno, T. & Rossi, J. J. Small interfering RNAs expressed from a Pol III promoter suppress the EWS/Fli-1 transcript in an Ewing sarcoma cell line. *Mol. Ther.* **7**, 811–816 (2003).
5. Hu-Lieskovan, S., Heidel, J. D., Bartlett, D. W., Davis, M. E. & Triche, T. J. Sequence-specific knockdown of EWS-FLI1 by targeted, nonviral delivery of small interfering RNA inhibits tumor growth in a murine model of metastatic Ewing's sarcoma. *Cancer Res.* **65**, 8984–8992 (2005).
6. Tanaka, K., Iwakuma, T., Harimaya, K., Sato, H. & Iwamoto, Y. EWS-Fli1 antisense oligodeoxynucleotide inhibits proliferation of human Ewing's sarcoma and primitive neuroectodermal tumor cells. *J. Clin. Invest.* **99**, 239–247 (1997).
7. Boulay, G. et al. Cancer-specific retargeting of BAF complexes by a prion-like domain. *Cell* **171**, 163–178 (2017).
8. Erkizan, H. V., Uversky, V. N. & Toretsky, J. A. Oncogenic partnerships: EWS-FLI1 protein interactions initiate key pathways of Ewing's sarcoma. *Clin. Cancer Res.* **16**, 4077–4083 (2010).
9. Riggi, N. et al. EWS-FLI1 utilizes divergent chromatin remodeling mechanisms to directly activate or repress enhancer elements in Ewing sarcoma. *Cancer Cell* **26**, 668–681 (2014).
10. Tomazou, E. M. et al. Epigenome mapping reveals distinct modes of gene regulation and widespread enhancer reprogramming by the oncogenic fusion protein EWS-FLI1. *Cell Rep.* **10**, 1082–1095 (2015).
11. Ahmed, N. S. et al. Fusion protein EWS-FLI1 is incorporated into a protein granule in cells. *RNA* **27**, 920–932 (2021).
12. Gangwal, K. et al. Microsatellites as EWS/FLI response elements in Ewing's sarcoma. *Proc. Natl Acad. Sci. USA* **105**, 10149–10154 (2008).
13. Kim, S., Denny, C. T. & Wisdom, R. Cooperative DNA binding with AP-1 proteins is required for transformation by EWS-Ets fusion proteins. *Mol. Cell. Biol.* **26**, 2467–2478 (2006).
14. Bilke, S. et al. Oncogenic ETS fusions deregulate E2F3 target genes in Ewing sarcoma and prostate cancer. *Genome Res.* **23**, 1797–1809 (2013).
15. Stegmaier, K. et al. Signature-based small molecule screening identifies cytosine arabinoside as an EWS/FLI modulator in Ewing sarcoma. *PLoS Med.* **4**, e122 (2007).
16. DuBois, S. G. et al. Phase II study of intermediate-dose cytarabine in patients with relapsed or refractory Ewing sarcoma: a report from the Children's Oncology Group. *Pediatr. Blood Cancer* **52**, 324–327 (2009).
17. Sankar, S. et al. Reversible LSD1 inhibition interferes with global EWS/ETS transcriptional activity and impedes Ewing sarcoma tumor growth. *Clin. Cancer Res.* **20**, 4584–4597 (2014).
18. Erkizan, H. V. et al. A small molecule blocking oncogenic protein EWS-FLI1 interaction with RNA helicase A inhibits growth of Ewing's sarcoma. *Nat. Med.* **15**, 750–756 (2009).
19. Grohar, P. J. et al. Ecteinascidin 743 interferes with the activity of EWS-FLI1 in Ewing sarcoma cells. *Neoplasia* **13**, 145–153 (2011).
20. Grohar, P. J. et al. Identification of an inhibitor of the EWS-FLI1 oncogenic transcription factor by high-throughput screening. *J. Natl Cancer Inst.* **103**, 962–978 (2011).
21. Grohar, P. J. et al. A phase I/II trial and pharmacokinetic study of mithramycin in children and adults with refractory Ewing sarcoma and EWS–FLI1 fusion transcript. *Cancer Chemother. Pharmacol.* **80**, 645–652 (2017).
22. Baruchel, S. et al. A phase 2 trial of trabectedin in children with recurrent rhabdomyosarcoma, Ewing sarcoma and non-rhabdomyosarcoma soft tissue sarcomas: a report from the Children's Oncology Group. *Eur. J. Cancer* **48**, 579–585 (2012).
23. Reed, D. et al. Phase 1 trial of seclidemstat (SP-2577) in patients with relapsed/refractory Ewing sarcoma. *J. Clin. Oncol.* **39**, 11514 (2021).
24. Felix, A. et al. Systematic review of phase-I/II trials enrolling refractory and recurrent Ewing sarcoma: actual knowledge and future directions to optimize the research. *Cancer Med.* **10**, 1589–1604 (2021).
25. Larsen, A. K., Galmarini, C. M. & D'Incalci, M. Unique features of trabectedin mechanism of action. *Cancer Chemother. Pharmacol.* **77**, 663–671 (2016).
26. Takebayashi, Y. et al. Antiproliferative activity of ecteinascidin 743 is dependent upon transcription-coupled nucleotide-excision repair. *Nat. Med.* **7**, 961–966 (2001).
27. Pommier, Y. et al. DNA sequence- and structure-selective alkylation of guanine N2 in the DNA minor groove by ecteinascidin 743, a potent antitumor compound from the Caribbean tunicate *Ecteinascidia turbinata*. *Biochemistry* **35**, 13303–13309 (1996).
28. Zewail-Foote, M. et al. The inefficiency of incisions of ecteinascidin 743–DNA adducts by the UvrABC nuclease and the unique structural feature of the DNA adducts can be used to explain the repair-dependent toxicities of this antitumor agent. *Chem. Biol.* **8**, 1033–1049 (2001).

29. Aune, G. J. et al. Von Hippel-Lindau-coupled and transcription-coupled nucleotide excision repair-dependent degradation of RNA polymerase II in response to trabectedin. *Clin. Cancer Res.* **14**, 6449–6455 (2008).
30. Soares, D. G. et al. Replication and homologous recombination repair regulate DNA double-strand break formation by the antitumor alkylator ecteinascidin 743. *Proc. Natl Acad. Sci. USA* **104**, 13062–13067 (2007).
31. Germano, G. et al. Role of macrophage targeting in the antitumor activity of trabectedin. *Cancer Cell* **23**, 249–262 (2013).
32. Lau, L. et al. A phase I and pharmacokinetic study of ecteinascidin-743 (Yondelis) in children with refractory solid tumors. A Children's Oncology Group study. *Clin. Cancer Res.* **11**, 672–677 (2005).
33. Scotlandi, K. et al. Effectiveness of Ecteinascidin-743 against drug-sensitive and -resistant bone tumor cells. *Clin. Cancer Res.* **8**, 3893–3903 (2002).
34. Harlow, M. L. et al. Lurbinectedin inactivates the Ewing sarcoma oncoprotein EWS-FLI1 by redistributing it within the nucleus. *Cancer Res.* **76**, 6657–6668 (2016).
35. Harlow, M. L. et al. Trabectedin inhibits EWS-FLI1 and evicts SWI/SNF from chromatin in a schedule-dependent manner. *Clin. Cancer Res.* **25**, 3417–3429 (2019).
36. Grohar, P. J. et al. Dual targeting of EWS-FLI1 activity and the associated DNA damage response with trabectedin and SN38 synergistically inhibits Ewing sarcoma cell growth. *Clin. Cancer Res.* **20**, 1190–1203 (2014).
37. Twelves, C. et al. Phase I and pharmacokinetic study of Yondelis (Ecteinascidin-743; ET-743) administered as an infusion over 1 h or 3 h every 21 days in patients with solid tumours. *Eur. J. Cancer* **39**, 1842–1851 (2003).
38. Hancock, J. D. & Lessnick, S. L. A transcriptional profiling meta-analysis reveals a core EWS-FLI gene expression signature. *Cell Cycle* **7**, 250–256 (2008).
39. Kinsey, M., Smith, R., Iyer, A. K., McCabe, E. R. & Lessnick, S. L. EWS/FLI and its downstream target NR0B1 interact directly to modulate transcription and oncogenesis in Ewing's sarcoma. *Cancer Res.* **69**, 9047–9055 (2009).
40. Richter, G. H. et al. EZH2 is a mediator of EWS/FLI1 driven tumor growth and metastasis blocking endothelial and neuro-ectodermal differentiation. *Proc. Natl Acad. Sci. USA* **106**, 5324–5329 (2009).
41. Zhang, H. F. et al. Proteomic screens for suppressors of anoikis identify IL1RAP as a promising surface target in Ewing sarcoma. *Cancer Discov.* **11**, 2884–2903 (2021).
42. Camoes, M. J. et al. Potential downstream target genes of aberrant ETS transcription factors are differentially affected in Ewing's sarcoma and prostate carcinoma. *PLoS ONE* **7**, e49819 (2012).
43. Orth, M. F. et al. Systematic multi-omics cell line profiling uncovers principles of Ewing sarcoma fusion oncogene-mediated gene regulation. *Cell Rep.* **41**, 111761 (2022).
44. Bading, J. R. & Shields, A. F. Imaging of cell proliferation: status and prospects. *J. Nucl. Med.* **49**, 64S–80S (2008).
45. Osgood, C. L. et al. ^{18}F-FLT positron emission tomography (PET) is a pharmacodynamic marker for EWS-FLI1 activity and Ewing sarcoma. *Sci. Rep.* **6**, 33926 (2016).
46. Perez-Ruixo, J. J. et al. Population pharmacokinetic meta-analysis of trabectedin (ET-743, Yondelis) in cancer patients. *Clin. Pharmacokinet.* **46**, 867–884 (2007).
47. Poggesi, I. et al. Population pharmacokinetics of trabectedin in adolescent patients with cancer. *Cancer Chemother. Pharmacol.* **84**, 707–717 (2019).
48. van Kesteren, C. et al. Clinical pharmacology of the novel marine-derived anticancer agent Ecteinascidin 743 administered as a 1- and 3-h infusion in a phase I study. *Anticancer Drugs* **13**, 381–393 (2002).
49. Attia, S. et al. A phase II trial of regorafenib in patients with advanced Ewing sarcoma and related tumors of soft tissue and bone: SARC024 trial results. *Cancer Med.* **12**, 1532–1539 (2023).
50. Italiano, A. et al. Cabozantinib in patients with advanced Ewing sarcoma or osteosarcoma (CABONE): a multicentre, single-arm, phase 2 trial. *Lancet Oncol.* **21**, 446–455 (2020).
51. Collier, A. B. et al. Outcome of patients with relapsed or progressive Ewing sarcoma enrolled on cooperative group phase 2 clinical trials: a report from the Children's Oncology Group. *Pediatr. Blood Cancer* **68**, e29333 (2021).
52. Duffaud, F. et al. Regorafenib in patients with advanced Ewing sarcoma: results of a non-comparative, randomised, double-blind, placebo-controlled, multicentre phase II study. *Br. J. Cancer* **129**, 1940–1948 (2023).
53. Demetri, G. D. et al. Efficacy and safety of trabectedin in patients with advanced or metastatic liposarcoma or leiomyosarcoma after failure of prior anthracyclines and ifosfamide: results of a randomized phase II study of two different schedules. *J. Clin. Oncol.* **27**, 4188–4196 (2009).
54. Osgood, C. L. et al. Identification of mithramycin analogues with improved targeting of the EWS-FLI1 transcription factor. *Clin. Cancer Res.* **22**, 4105–4118 (2016).

Patrick J. Grohar[1] ✉, Rachel Heise[2], Mary Frances Wedekind[3], Karla Ballman[4], Leo Mascarenhas[5], Steven G. DuBois[6], Robert G. Maki[7], Elissa A. Boguslawski[1], Jenna M. Gedminas[8], Elizabeth R. Wilson[9], Elaine Thomas[3], Blair Segers[9], Lea F. Surrey[10], Cora Ricker[6], Kelly Klega[6], Fariba Navid[11], Gretchen Y. Lam[12], Stephanie The[12], Rebecca Kaufman[9], Ryan D. Roberts[13], Masanori Hayashi[14], Esther Mena[15], Lindsey Overman[16], Cody Peer[17], Keith Schmidt[17], Mark S. Diamond[18], William D. Figg[17], Rochelle Bagatell[9], M. Liza Lindenberg[15], Peter L. Choyke[15], Brian D. Crompton[6], Brigitte C. Widemann[3], John W. Glod[3], Theodore W. Laetsch[9], Denise K. Reinke[19] & Rashmi Chugh[19]

[1]Division of Pediatric Hematology/Oncology, University of Michigan Medical School, C.S. Mott Children's Hospital, Rogel Cancer Center, Ann Arbor, MI, USA. [2]Weill Cornell Medicine, New York, NY, USA. [3]Pediatric Oncology Branch, National Cancer Institute, National Institutes of Health, Bethesda, MD, USA. [4]Mayo Clinic, Rochester, MN, USA. [5]Guerin Children's and Cedars Sinai Cancer, Cedars Sinai Health Sciences University, Los Angeles, CA, USA.

[6]Dana-Farber/Boston Children's Cancer and Blood Disorders Center and Harvard Medical School, Boston, MA, USA. [7]Memorial Sloan-Kettering Cancer Center, New York, NY, USA. [8]Division of Pediatric Hematology/Oncology, Department of Pediatrics, University of Iowa, Iowa City, IA, USA. [9]Division of Oncology, Children's Hospital of Philadelphia, Philadelphia, PA, USA. [10]Department of Pathology and Laboratory Medicine, Children's Hospital of Philadelphia, Philadelphia, PA, USA. [11]Cancer and Blood Disease Institute, Children's Hospital of Los Angeles, Department of Pediatrics, Keck School of Medicine, University of Southern California, Los Angeles, CA, USA. [12]Department of Biostatistics, University of Michigan, Ann Arbor, MI, USA. [13]Department of Pediatrics, Center for Childhood Cancer, Nationwide Children's Hospital, Ohio State University, Columbus, OH, USA. [14]Department of Pediatrics, University of Colorado Anschutz Medical Campus and Center for Cancer and Blood Disorders, Children's Hospital of Colorado, Aurora, CO, USA. [15]Molecular Imaging Program, National Cancer Institute, National Institutes of Health, Bethesda, MD, USA. [16]Sarcoma Alliance for Research through Collaboration, Ann Arbor, MI, USA. [17]Clinical Pharmacology Program, National Cancer Institute, National Institutes of Health, Bethesda, MD, USA. [18]Department of Medicine, Perelman School of Medicine, University of Pennsylvania, Philadelphia, PA, USA. [19]University of Michigan Rogel Cancer Center, Ann Arbor, MI, USA. ✉e-mail: grohar@med.umich.edu

Methods

Ethics approval and consent

WCG Connexus was the central institutional review board (IRB) for this study. IRB approval of the study at each site was maintained throughout the conduct of the trial. All sites used IRB-approved informed consent. All patients and/or legal guardians were required to provide consent or assent.

Patients

Patients aged >10 years (Ph1) or >6 years (Ph2) with relapsed, treatment-refractory ES and documented EWS::FLI1 fusion/breakpoint were enrolled. Patients were required to have adequate performance status (ECOG of 0–2 or Lansky >50) and adequate organ function with evaluable (Ph1) or measurable (Ph2) disease as defined by RECIST 1.1. Prior irinotecan was allowed, but patients were excluded if they previously received trabectedin. Patients >18 years of age were required to undergo tumor biopsy at study entry and after administration of trabectedin unless contraindicated and/or approved by the overall study principal investigator. Sex and gender as a biological variable were self-reported and not included in the study design due to the rarity of the disease (as in similar studies from consortia). No post hoc sex or gender analysis was performed due to the limited sample size.

Study design

SARC037 (ClinicalTrials.gov identifier: NCT04067115) is a Ph1/Ph2 multicenter study conducted by the Sarcoma Alliance for Research through Collaboration (SARC) to evaluate the safety of trabectedin administered as 1-hour infusion in patients with ES in combination with low-dose irinotecan and ^{18}F-FLT imaging. No compensation was provided to the participants. Data were collected centrally in an electronic data capture system (Medidata). The protocol will be provided to investigators upon reasonable request. The primary endpoint of the Ph1 portion was to determine the recommended dose of trabectedin in combination with low-dose irinotecan; the primary endpoint of the Ph2 portion was the confirmed tumor ORR per RECIST 1.1. Secondary objectives in Ph1 and Ph2 included estimation of the tumor response rate per RECIST 1.1, PFS, duration of response and 6-month PFS rate. An additional secondary objective in Ph1 was to determine the ^{18}F-FLT PET avidity of ES tumors. The Ph1 portion was a 3 + 3 design with escalation first of trabectedin and then irinotecan. The Ph2 was a Simon minimax two-stage design requiring one objective response in the first seven patients to proceed to the second stage and enroll an additional 11 patients. The primary Ph2 endpoint was ORR and was defined as positive with four or more objective responses in the 18 patients enrolled in the Ph2 portion (one-sided α of 0.089 and 80% power).

Statistical analysis

In the Ph1 portion, patients were enrolled until the recommended dose was obtained, with a minimum number of three patients and a maximum of 30 patients. For the Ph2 portion, a Simon minimax two-stage design was used to determine the sample size. A historical ORR value of 10% was used, and this study was powered to detect an ORR of 30% or higher, with a one-sided α of 0.089 and 80% power. ORR was defined as the number of patients with a complete response or partial response, divided by the total number of patients enrolled who received at least one dose of protocol treatment. This was estimated with a binomial point estimate and 95% confidence interval. Patients without a follow-up tumor assessment were considered a non-response.

Secondary endpoints for the Ph1 and Ph2 portions of the trial were calculated in all patients who started treatment. PFS was defined as the time from study enrollment until disease progression or death, whichever occurred first. Patients who were alive at the time of analysis without documented progression were censored at the time of their last disease evaluation. The median PFS and 95% confidence interval as well as 6-month PFS rate were estimated with a Kaplan–Meier estimator. Duration of response was defined as the time between first meeting measurement criteria for complete response or partial response until recurrent or progressive disease is documented; this was estimated using a Kaplan–Meier estimator.

The safety analysis was conducted on all patients who received at least one dose of study drug. The frequency and grade of all adverse events were reported using standard Common Terminology Criteria for Adverse Events (CTCAE) version 5.0. Adverse events that occurred in at least 15% of patients were summarized, including the maximum grade adverse event for each event experienced by the patient.

Pharmacokinetics

Pharmacokinetic samples were collected after the first dose at nominal times of predose, 30 minutes, 1 hour, 3 hours, 5 hours, 24 hours, 48 hours and 168 hours after end of infusion, with variability allowed around these timepoints. A validated liquid chromatography–tandem mass spectrometry (LC–MS/MS) assay with a lower limit of quantification (LLOQ) of 0.05 ng ml^{-1} was used to quantitate trabectedin plasma concentrations. Mid-infusion and end-of-infusion trabectedin plasma concentrations were simulated via a previously published population pharmacokinetic model[46,47] using NONMEM (ICON plc). Quantitated and model-predicted trabectedin plasma concentrations were combined to generate concentration–time profiles for each patient. Pharmacokinetic parameters were estimated using a non-compartmental analysis (NCA) using Phoenix WinNonlin 8.5 (Certara), validated per FDA 21 CFR Part 11. C_{max} and time of C_{max} (T_{max}) values were assessed as observations. The AUC was determined using the linear up/log down trapezoidal rule from the initial infusion start time through the last measured (AUC_{last}). C_{max} and AUC were also normalized by dose (that is, C_{max}/dose and AUC/dose).

ctDNA

Blood samples were collected at up to six timepoints, including precycle 1, cycle 1 day 2, cycle 1 day 8, precycle 2, end of treatment and progression. For each timepoint, samples underwent DNA extraction, library preparation, ultra-low-pass whole-genome sequencing (ULP-WGS), custom panel sequencing (TranSS-Seq) and data analysis as previously described[55] with the following exceptions: whole blood was collected in PAXgene Blood ccfDNA Tubes (BD Biosciences), stored and shipped at 4 °C, and plasma was double spun prior to storing at −80 °C until extraction.

EWS::FLI1 transcriptome analysis

Bulk RNA sequencing analysis. RNA was purified using mechanical disruption and column purification. Reads were aligned to hg38 with STAR version 2.7.3a and quantified with RSEM 1.3.3 using GENCODE 31 annotations. After quantification, induced and repressed targets were identified, and $\log_2$ fold change was calculated.

Spatial transcriptomics

Formalin-fixed paraffin-embedded (FFPE) slides were sectioned, and regions were identified and subjected to spatial sequencing on the Visium HD platform (10x Genomics). The data were processed on 10x Space Ranger software for read alignment, UMI counting and normalization by the Advanced Genomics Core at the University of Michigan. Data were log normalized to display UMI counts normalized to total UMI counts per cells, separated into tumor and normal using *k*-means setting at 2 and compared between samples as the average expression of the feature list of EWS::FLI1 targets described below. Expression was visualized on the Loupe Browser version 8 with settings as LogNormalized and Feature Avg.

EWS::FLI1 target gene lists

A composite feature list was generated by literature review of 10 well-established EWS::FLI1 target genes associated with GGAA microsatellites: *NR0B1*, *IL1RAP*, *EZH2*, *CAV1*, *AKAP7*, *CACNB2*, *RCOR1*, *FCGRT*, *FEZF1* and *FOCAD*[12,39–42]. An additional list of EWS::FLI1 microsatellite-bound

induced targets was generated from recently published CUT&Tag data of EWS::FLI1. Peaks were called from CUT&Tag data using SEACR (version 1.3) to return the top 1% of peaks. BEDTools multiinter was used to generate a list of consensus peaks from the three control replicates, followed by 'awk' to filter for regions that were at least 24 bp long. BEDTools getfasta was then used with these regions and a FASTA file of the hg38 genome reference to extract the sequences of the consensus peaks. Tandem Repeats Finder (version 4.09.1) was used to identify regions with 4-bp repeats, followed by 'awk' to identify sequences with at least six GGAA repeats. To identify which genes are most closely associated with each repeat, the hg38 annotation file was first filtered to transcription start sites (TSSs) of the Lessnick list of EWS::FLI1 induced or repressed targets[38]. BEDTools window was then used to identify TSSs in the filtered annotation file within 250 kbp of the previously identified GGAA-containing peaks ($n = 175$). This distance was chosen as representing less than the published average distance to target in an aggregate analysis of 18 cell lines[43].

Aggregate and individual patient analysis

Analysis of the spatial transcriptomics data was performed with Seurat version 5.3.0 on R version 4.4.0. Downstream analyses were performed on the 8-µm-resolution data. Each sample was separately normalized using the NormalizeData function with a scale factor of 10,000, followed by extracting the top 2,000 variable features using FindVariableFeatures and scaling using ScaleData. Sketching was then applied to each sample, using a random subsample of 5,000 spots each. Then, the sketched samples were merged, and feature selection, scaling and principal component analysis (PCA) were run on the merged sketched dataset. Integration was performed using the RunHarmony function, with the patient origin as the batch variable. The sketched data were then projected back to the full dataset. To determine the relative expression of the genes in the microsatellite list extracted from the CUT&Tag data, the AddModuleScore function was used to score each gene set. One-sided Wilcoxon rank-sum tests were performed to assess whether the median expression was higher in pretreatment samples compared to posttreatment samples, across all samples and within each sample. The Benjamini–Hochberg method was applied to control the false discovery rate in multiple hypothesis testing.

^{18}F-FLT PET

^{18}F-FLT was administered intravenously at a weight-based dose of 0.07 mCi per kilogram approximately 60 minutes prior to whole-body scanning on a GE MI Discovery PET/CT in three-dimensional mode. Low-dose, non-contrast-enhanced computed tomography scan was acquired for attenuation correction and anatomical localization, and PET was reconstructed through iterative time-of-flight algorithms. Images were obtained at baseline, prior to or 1 day after the first dose of irinotecan and after treatment. Volumes of interest were drawn on tumors using MIM Software, with acquisition of PET parameters including standardized uptake values (SUVs) and tumor volume for quantitative analysis.

Reporting summary

Further information on research design is available in the Nature Portfolio Reporting Summary linked to this article.

Data availability

Data were obtained with appropriate consents and have been submitted to the Gene Expression Omnibus in an anonymized fashion with accession number GSE322640.

References

55. Shulman, D. S. et al. Phase 2 trial of palbociclib and ganitumab in patients with relapsed Ewing sarcoma. *Cancer Med.* **12**, 15207–15216 (2023).

Acknowledgements

We gratefully acknowledge William 'Bill' Timmer, posthumously, the former Program Director of the National Cancer Institute (NCI), whose guidance and support launched this project. We thank all the patients and their families who participated in this study and, importantly, those patients who contributed their tissues and blood samples to help us better understand ES. The authors are grateful for the support from the Punchard family. This project has been funded, in whole or in part, with funding from the National Institutes of Health (NIH)/NCI (U01CA236220) and Janssen Scientific Affairs, LLC. Correlative biology was supported by non-overlapping funding from the U01, the V Foundation and the 1Million4Anna Foundation. The funders had no role in study design, data collection and analysis, decision to publish or preparation of the manuscript. Additional support was provided by the Pediatric Oncology Branch and the intramural program at the NCI for B.C.W., J.W.G., E.T. and M.F.W. and by grant ZIE BC 011516. Preclinical work to develop and support the conclusions of the study was supported by St. Baldrick's Foundation, NIH/NCI (R01CA188314 and R01CA283058) and Alex's Lemonade Stand Foundation (ALSF). ALSF provided additional support for the conduct of the study (T.L., J.G. and B.S.). Spatial transcriptomics was carried out in the Advanced Genomics Core at the University of Michigan and was supported by the NCI under award number P30CA046592 by the use of the spatial analysis shared resource. Pharmacokinetics was supported by the intramural program at the NCI and the ZIC SC 006537 grant. The authors would like to acknowledge the contributions of O. Arisa and K. Olubanjo to the pharmacokinetic analysis. ^{18}F-FLT PET imaging was supported by the Intramural Imaging Program at the NCI (ZIA BC 010656 grant). The content of this publication does not necessarily reflect the views or policies of the US Department of Health and Human Services nor does mention of trade names, commercial products or organizations imply endorsement by the US Government. This research was supported in part by the Intramural Research Program of the NIH. The contributions of NIH authors were made as part of their official duties as NIH federal employees, are in compliance with agency policy requirements and are considered works of the US Government. However, the findings and conclusions presented in this paper are those of the authors and do not necessarily reflect the views of the NIH or the US Department of Health and Human Services.

Author contributions

Conceptualization: P.J.G., R.C., D.K.R. and B.C.W. Methodology/design: P.J.G., R.C., D.K.R., R.H., K.B., R.D.R., M.H., B.D.C., C.P., W.D.F., K.S., P.L.C., T.W.L., J.W.G., R.B., M.L.L., E.A.B., L.F.S. and L.M. Validation: P.J.G., R.C., R.H. and K.D. Formal analysis: P.J.G., R.C., D.K.R., R.H., K.B., R.K., S.T., G.L., C.R., K.K., B.C.D., K.S., E.R.W., E.A.B., R.D.R., M.F.W., J.W.G., M.L.L., E.M., L.M. and L.F.S. Investigation/data acquisition: all authors. Data curation: P.J.G., R.C., D.K.R., L.O., R.H. and E.R.W. Writing—original draft: P.J.G., R.C., D.K.R., B.C.W., J.W.G., T.W.L., R.H., E.A.B., B.D.C., K.S., W.D.F., M.F.W. and R.D.R. Writing—review and editing: all authors. Visualization: P.J.G., R.C., D.K.R., E.A.B., R.H., G.L., S.T., R.K., B.C.D., C.R.K. and K.K. Supervision: P.J.G., R.C., D.K.R., J.W.G., M.L.L., W.D.F., B.D.C., E.A.B. and K.B. Funding acquisition: P.J.G., R.C., D.K.R., B.C.W. and T.W.L. All authors approved the final version of the manuscript.

Competing interests

P.J.G. has received honoraria for grant review and a symposium from the Pharma Mar Foundation; served as advisor for OrphAI therapeutics with options and honoraria for advisory board participation for Jazz and Inhibrx; and received support to his institution from Janssen Scientific Affairs, LLC. L.M. has received honoraria for work products from Novartis; received consultant, travel and accommodation compensation for scientific presentations from Bayer; and has uncompensated relationships with the Children's Oncology Group (COG) Foundation, the COG Research Foundation, the COG Bone

Tumor Committee and the Pablove Foundation. S.G.D. has provided consulting for Bayer, Amgen, Jazz Pharmaceuticals, InhibRx, EMD Serono and Merck. R.G.M. has received consulting fees or honoraria from Boehringer Ingelheim, Deciphera, Ipsen, Physicians' Education Resource, the American Board of Internal Medicine, the American Society for Clinical Oncology and Peel Therapeutics and receives royalties from UpToDate for sarcoma-related content and stock from Peel Therapeutics for work with Peel. T.W.L. participates in consulting/advisory boards for Advanced Microbubbles, OrphAI Therapeutics, Bayer, GlaxoSmithKline, ITM Oncologics and Jazz Pharmaceuticals and receives research support to his institution from Bayer, Pfizer, Eli Lilly and Exelixis. D.K.R. has received honoraria for advisory boards from Boehringer Ingelheim and Merck. R.C. has done advisory work for Deciphera, Recordati and Cogent Biosciences and receives royalties from UpToDate with all research support going to her institution. R.H., M.F.W., K.B., E.A.B., J.M.G., E.R.W., E.T., B.S., L.F.S., C.R., K.K., F.N., G.L., S.T., R.K., R.D.R., M.H., E.M., L.O., C.P., K.S., M.S.D., W.D.F., R.B., M.L.L., P.L.C., B.D.C., B.C.W. and J.G.G. declare no competing interests.

Additional information

Extended data is available for this paper at https://doi.org/10.1038/s41591-026-04340-7.

Supplementary information The online version contains supplementary material available at https://doi.org/10.1038/s41591-026-04340-7.

Correspondence and requests for materials should be addressed to Patrick J. Grohar.

Peer review information *Nature Medicine* thanks Thibaud Valentin and the other, anonymous, reviewer(s) for their contribution to the peer review of this work. Primary Handling Editor: Ulrike Harjes, in collaboration with the *Nature Medicine* team.

https://doi.org/10.1038/s41591-026-04340-7

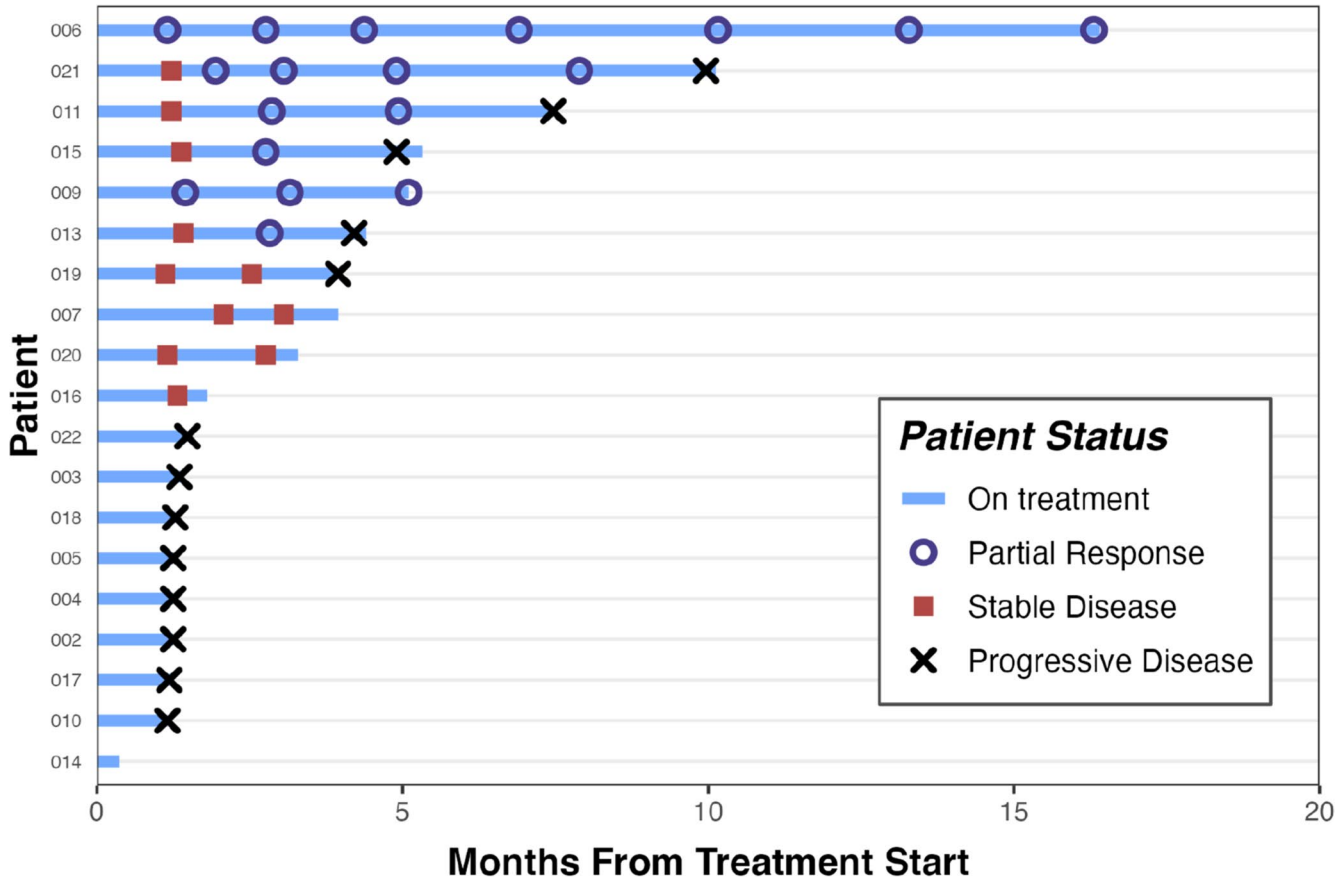

Extended Data Fig. 1 | Sustained patient responses in Phase I. Swimmer plot of patients enrolled in the phase I portion of SARC037 showing response as a function of time in months from the start of therapy by patient.

https://doi.org/10.1038/s41591-026-04340-7

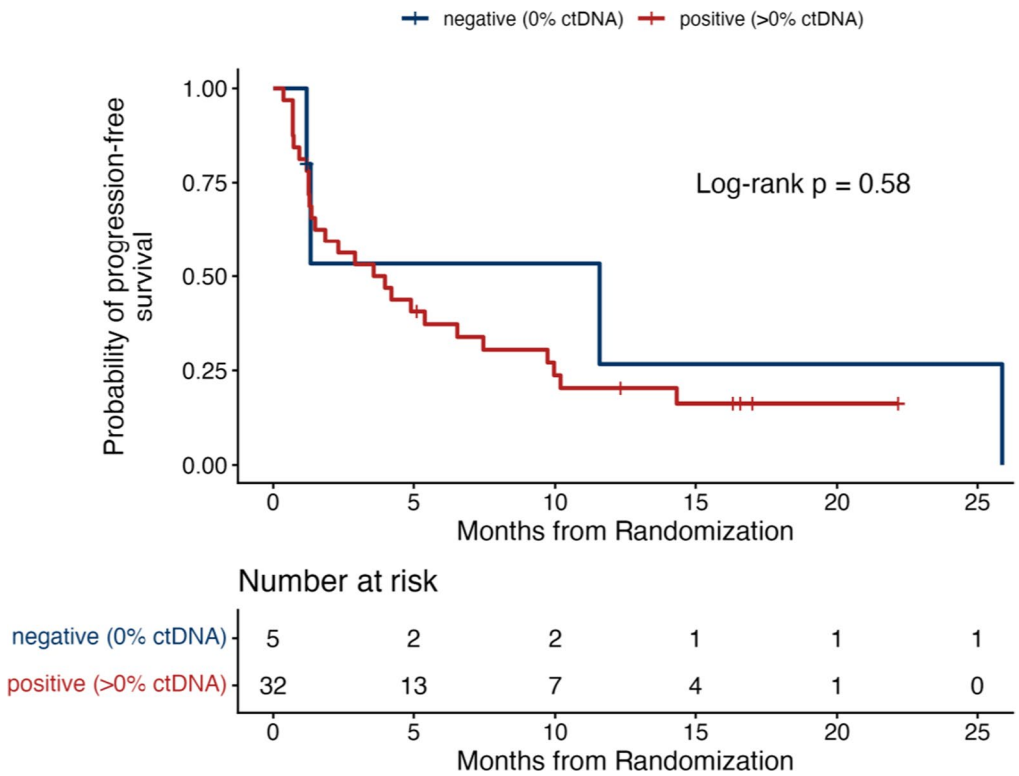

Extended Data Fig. 2 | Baseline ctDNA of patients in phase I/II. Progression free survival (%) as function of time on study in years. Patients are stratified by those with no detectable ctDNA on day 0 (prior to starting therapy; blue, n = 5) vs. those with detectable ctDNA on day 0 (prior to starting therapy); red; n = 32). There is no significant difference ($P = 0.58$) in outcome in patients stratified by detectable circulating tumor DNA on day 0. Analysis was performed using the log-rank test ($\chi^2 = 0.31, 1$ df), with a hazard ratio of 1.41 (95% CI 0.42 to 4.68).

https://doi.org/10.1038/s41591-026-04340-7

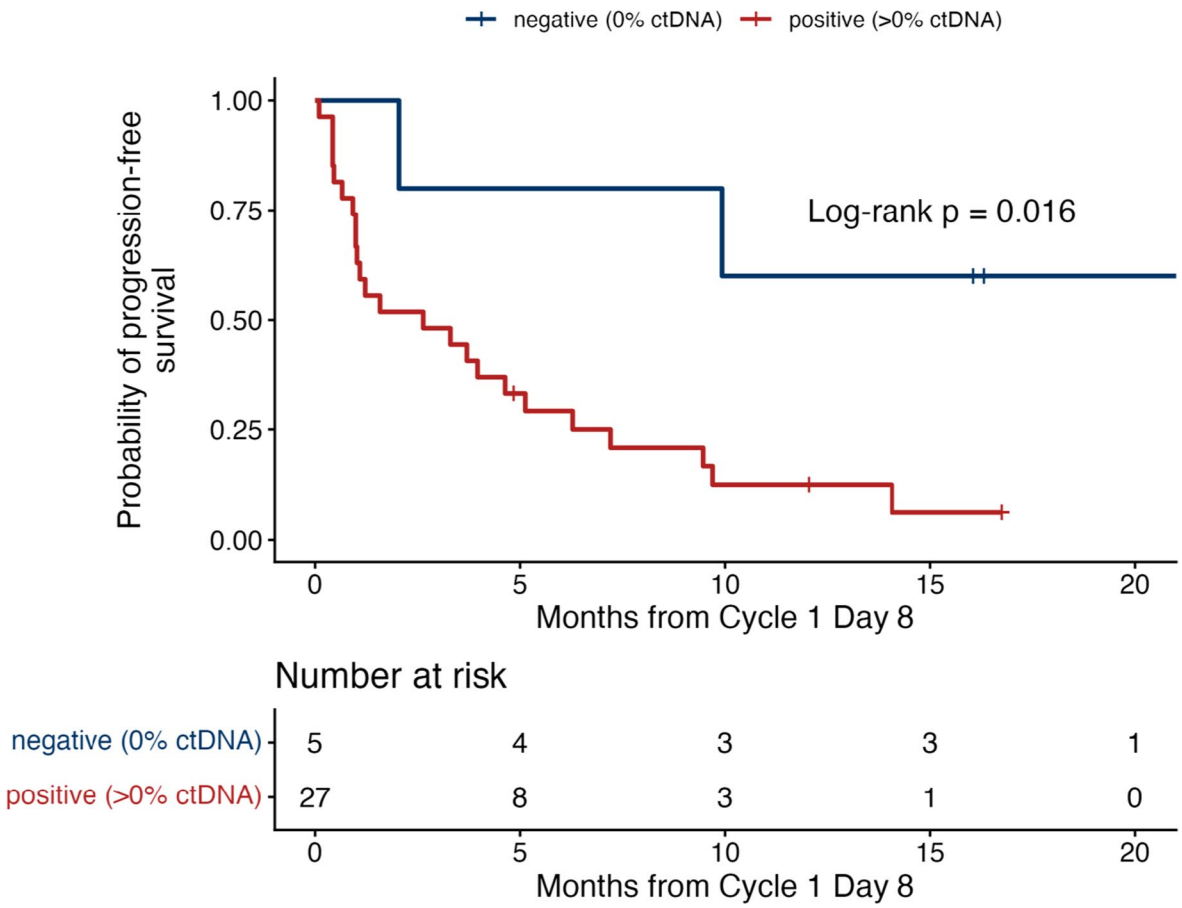

Extended Data Fig. 3 | Day 8 ctDNA of patients in phase I/II excluding those with no detectable baseline ctDNA. Kaplan-Meier survival curves featuring survival as a function of time in months from cycle 1 for all patients in Ph1 and Ph2 with detectable ctDNA at baseline stratified by non-detectable (blue, n = 5) and detectable ctDNA (red, n = 27) on day 8 ($P = 0.016$).

https://doi.org/10.1038/s41591-026-04340-7

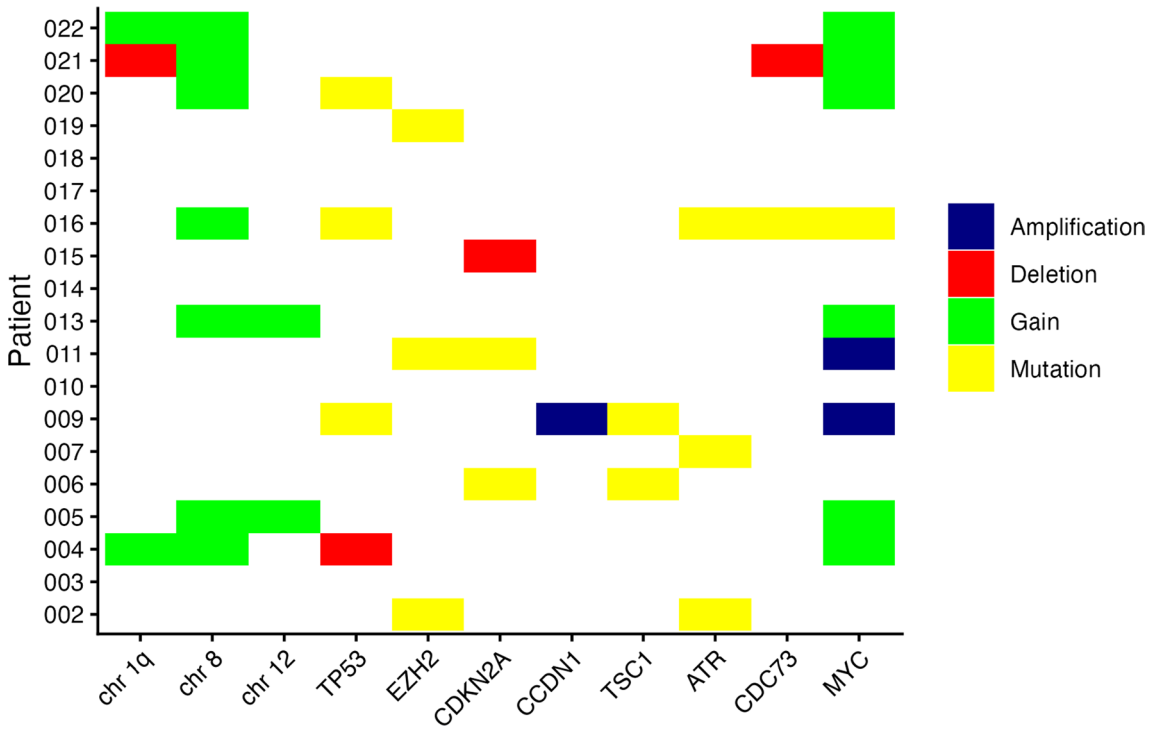

Extended Data Fig. 4 | Oncoplot of patients enrolled in phase I. Oncoplot showing frequency of mutations in individual patients (y-axis) as a function of mutation (x-axis) and type either amplification (blue), deletion (red), copy number gain (green) or mutation (yellow).

https://doi.org/10.1038/s41591-026-04340-7

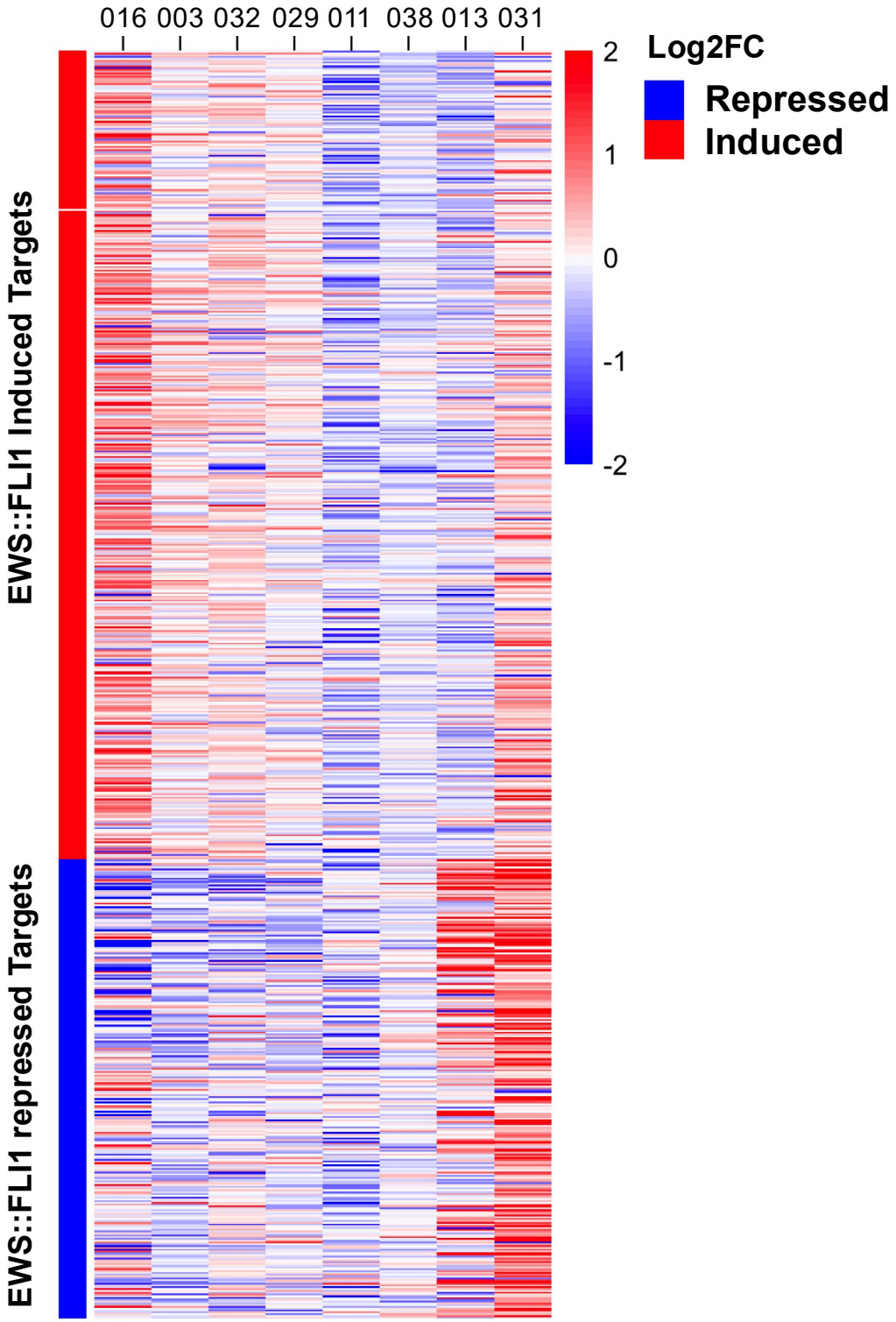

Extended Data Fig. 5 | Suppression of EWS::FLI1 in 3 of 8 patients in phase I/II. Heatmap demonstrating Log2FC in expression (Post-treatment to Pre-treatment; Red is up, blue is down) of the Lessnick List of EWS::FLI1 induced (red line Y-axis, top) or EWS::FLI1 repressed (blue line Y-axis, bottom) targets. Clear reversal of expression is evident for 013, 38, 11 and less penetrant reversal for the other patients. Lessnick list of EWS::FLI1 induced and suppressed targets used for the analysis (see text for reference).

https://doi.org/10.1038/s41591-026-04340-7

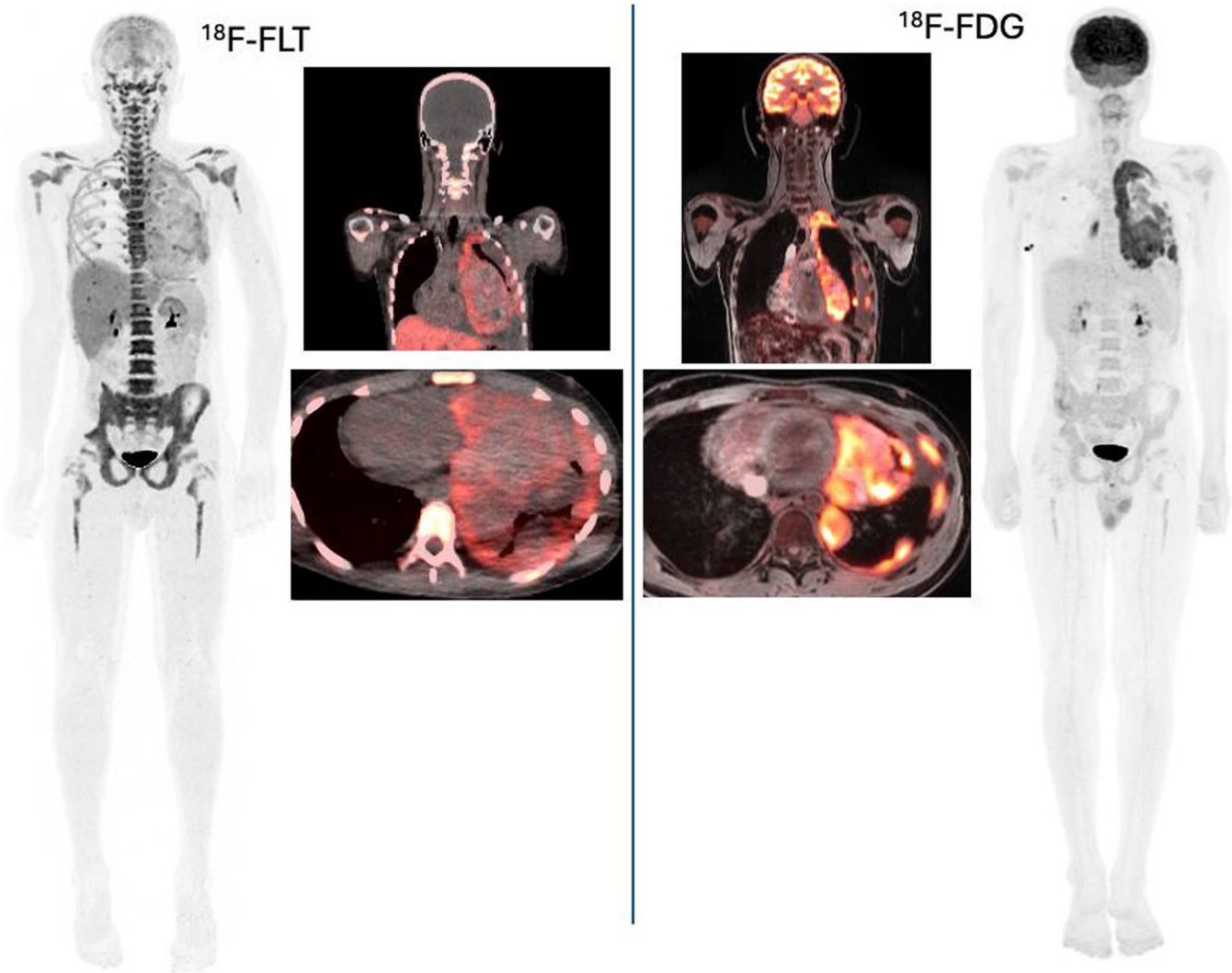

Extended Data Fig. 6 | Comparison of 18F-FDG and 18F-FLT PET signal. Similar sensitivity of ^{18}F-FLT and ^{18}F-FDG in the same patient. Note the ^{18}F-FLT PET scan was 7 weeks after the ^{18}F-FDG scan and so has a higher tumor burden. Similar sensitivity but altered distribution of background is seen with ^{18}F-FLT favoring the bone marrow while ^{18}F-FDG favors the brain.

https://doi.org/10.1038/s41591-026-04340-7

A

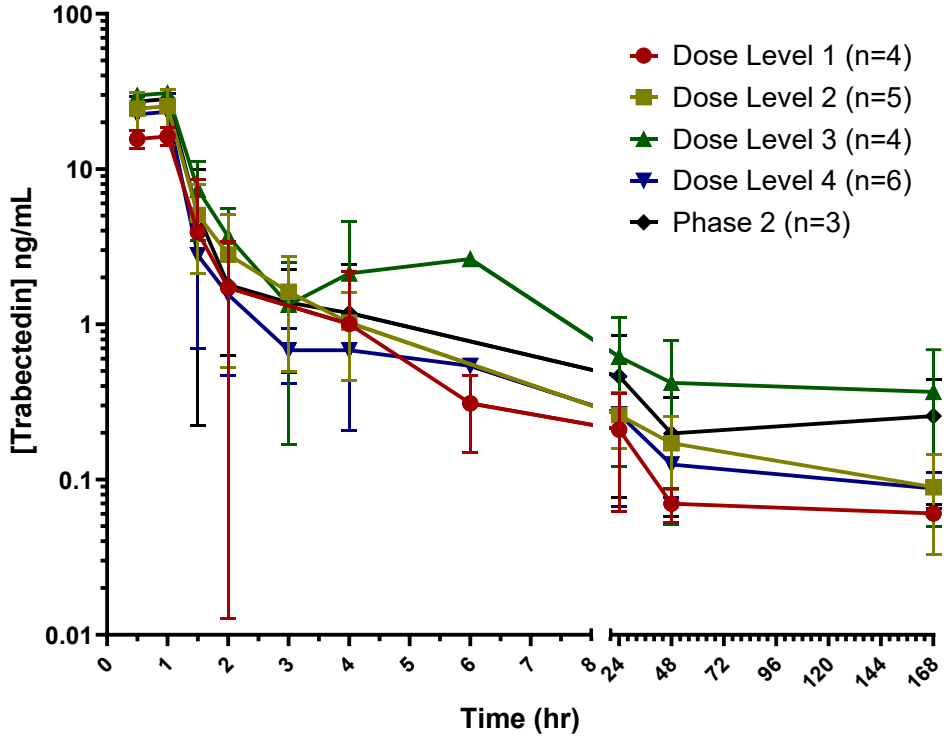

B

Dose Level	T_{max} (hr)	C_{max} (ng/mL)	C_{max}/Dose (ng/mL/mg)	AUC (hr*ng/mL)	AUC/Dose (hr*ng/mL/mg)
Dose Level 1 (n=4) **Trabectedin 0.8 mg/m²** **Irinotecan 25 mg/m²**	1.04 (1.02–1.07)	16.24 (2.13)	12.96 (0.38)	44.80 (17.78)	36.99 (18.52)
Dose Level 2 (n=5) **Trabectedin 1.0 mg/m²** **Irinotecan 25 mg/m²**	1.03 (1.00-1.10)	25.39 (6.97)	14.06 (0.56)	59.80 (8.76)	35.50 (13.32)
Dose Level 3 (n=4) **Trabectedin 1.1 mg/m²** **Irinotecan 25 mg/m²**	1.05 (1.00-1.17	30.86 (3.03)	13.45 (1.46)	130.4 (70.49)	57.70 (32.42)
Dose Level 4 (n=6) **Trabectedin 1.0 mg/m²** **Irinotecan 30 mg/m²**	1.00 (0.98-1.00)	23.43 (7.03)	13.21 (1.88)	54.18 (13.16)	32.31 (9.77)
Phase II (n=3) **Trabectedin 1.0 mg/m²** **Irinotecan 25 mg/m²**	1.02 (0.93-1.08)	28.31 (2.23)	14.15 (1.11)	88.65 (36.06)	44.32 (18.03)
DL2 + DL4 + Phase 2 (n=14) **Trabectedin 1.0 mg/m²**	1.01 (0.93-1.10)	25.17 (6.20)	13.72 (1.36)	63.57 (21.94)	36.03 (12.79)

Extended Data Fig. 7 | Pharmacokinetic profiling of patients in phase I. (**a**) Mean concentration (mean +/- SD) vs. time profiles of trabectedin by dose level for patients enrolled at 4 different dose levels, DL1 (0.8 mg/m² T (trabectedin)(day 1) 25 mg/m² I (Irinotecan)(days 2 & 4)), DL2 (1.0 mg/m² T (day 1) 25 mg/m² I (days 2 & 4)), DL3 (1.1 mg/m² T (day 1) 25 mg/m² I (days 2 & 4)) DL4 (1.0 mg/m² T (day 1) 30 mg/m² I (days 2 & 4)), and all patients who got 1.0 mg/m² trabectedin and Pk profiling. (**b**) Table summarizing non-compartmental analysis of trabectedin pharmacokinetics for patients on phase I.

https://doi.org/10.1038/s41591-026-04340-7

Extended Data Table 1 | Adverse events at the RP2D in >15% of patients

	N = 23			
Adverse Event	Grade 1 or 2	Grade 3	Grade 4	Overall
Blood and lymphatic system				
ANEMIA	8 (35)	6 (26)	—	14 (61)
Cardiac disorders				
SINUS TACHYCARDIA	5 (22)	—	—	5 (22)
Gastrointestinal disorders				
ABDOMINAL PAIN	6 (26)	—	—	6 (26)
CONSTIPATION	10 (43)	—	—	10 (43)
DYSPEPSIA, BELCHING, GASTRITIS, GERD	5 (22)	—	—	5 (22)
LOOSE STOOL/DIARRHEA	9 (39)	1 (4.3)	—	10 (43)
NAUSEA	21 (91)	1 (4.3)	—	22 (96)
VOMITING	14 (61)	—	—	14 (61)
General disorders and administration site conditions				
FATIGUE/MALAISE	14 (61)	1 (4.3)	—	15 (65)
FEVER	4 (17)	—	—	4 (17)
Infections and infestations				
COUGH/COLD/UPPER RESPIRATORY INFECTION	5 (22)	—	—	5 (22)
Laboratory findings				
ALANINE AMINOTRANSFERASE INCREASED	4 (17)	9 (39)	3 (13)	16 (70)
ALKALINE PHOSPHATASE INCREASED	5 (22)	—	—	5 (22)
ASPARTATE AMINOTRANSFERASE INCREASED	11 (48)	3 (13)	2 (8.7)	16 (70)
BLOOD BICARBONATE DECREASED	5 (22)	—	—	5 (22)
BLOOD LACTATE DEHYDROGENASE INCREASED	10 (43)	—	—	10 (43)
CPK INCREASED	4 (17)	2 (8.7)	—	6 (26)
CREATININE INCREASED	7 (30)	—	—	7 (30)
LYMPHOCYTE COUNT DECREASED	7 (30)	5 (22)	1 (4.3)	13 (57)
NEUTROPHIL COUNT DECREASED	3 (13)	4 (17)	10 (43)	17 (74)
PLATELET COUNT DECREASED	4 (17)	4 (17)	8 (35)	16 (70)
WHITE BLOOD CELL DECREASED	2 (8.7)	6 (26)	7 (30)	15 (65)
Metabolism and nutrition disorders				
ANOREXIA	7 (30)	—	—	7 (30)
HYPERGLYCEMIA	7 (30)	—	—	7 (30)
HYPERPHOSPHATEMIA	4 (17)	1 (4.3)	—	5 (22)
HYPOKALEMIA	7 (30)	—	—	7 (30)
HYPONATREMIA	8 (35)	—	—	8 (35)
HYPOPHOSPHATEMIA	5 (22)	—	—	5 (22)
Musculoskeletal and connective tissue disorders				
BACK PAIN/BONE PAIN/PAIN IN EXTREMITY	7 (30)	1 (4.3)	—	8 (35)
Nervous system disorders				
HEADACHE	10 (43)	—	—	10 (43)
PARESTHESIA	5 (22)	—	—	5 (22)
Respiratory, thoracic and mediastinal disorders				
COUGH	9 (39)	—	—	9 (39)
DYSPNEA	4 (17)	1 (4.3)	—	5 (22)
RHINORRHEA	4 (17)	—	—	4 (17)
Vascular disorders	8 (35)	—	—	8 (35)
HYPERTENSION	6 (26)	—	—	6 (26)

https://doi.org/10.1038/s41591-026-04340-7

Extended Data Table 2 | Clinical and molecular factors associated with patient response

A

Characteristic	Responders n = 9	Non-responders N = 14	*P-value*
Baseline sum of tumor diameters (mm)*	45 (31,62)	51 (35, 84)	0.5
Number of prior lines of therapy**	3 (3, 5)	4 (3,4)	0.7
Prior irinotecan***	5 (56%)	9 (64%)	>0.9
Alternative exon usage***	4 (44%)	6 (43%)	>0.9

B

Molecular Change	Responders; n (%)	Non-responders; n (%)
Copy Number Variants		
Chromosome 2 or 1	3 (33)	2 (14)
Chromosome 8	2 (22)	6 (43)
Chromosome 12	1 (11)	1 (7)
Other Copy Number Variants	4 (44)	4 (29)
Mutations		
TP53	1 (11)	1 (7)
EZH2	0 (0)	1 (7)
CDKN2A	2 (22)	0 (0)
STAG2	0 (0)	1 (7)
ATM	1 (11)	1 (7)
CCND1	1 (11)	0 (0)
TSC1	2 (22)	0 (0)
SMARCA4	2 (22)	0 (0)
MYC/MYCN	5 (56)	6 (43)
Notch 1-3 tier III	3 (33)	0 (0)

Molecular and clinical factors (characteristic) and associated number of patients (percentage), stratified by responder (n=9) vs non-responder (n=14) and associated *P*-value. Data is median (Q1, Q3) percentage. P is Wilcoxon exact, rank sum or Fisher's exact test defined by RECIST objective response for all patients treated at the RP2D. Alternative exon usage represents patient tumors with EWSR1::FLI1 fusion proteins that were non-type I (exon 7 EWSR1, Exon 6 FLI1) or non-type II (Exon 7 EWSR1, Exon 5 FLI1) fusion proteins. **b**. Copy number variants or mutations associated with number (percentage) of responder and non-responder defined by RECIST criteria for all patients treated at the RP2D. The only statistically significant factor association between response and mutation is NOTCH (*P*=0.047).

https://doi.org/10.1038/s41591-026-04340-7

Extended Data Table 3 | EWS::FLI1 alternative exon usage as function of number of prior lines of therapy

Number of Prior Lines of therapy	Alternate Exon Usage (n =10)	No Alternative Exons (n =13)	*P-value*
Less than 4	2 (20%)	9 (69%)	0.036
Greater than or equal to 4	8 (80%)	4 (31%)	

Non-type I or II (alternative exons usage, N=10) vs. type I,II (No alternative exon usage, N=13) and associated *P*-value for all patients treated at the RP2D stratified by number of prior lines of therapy either greater or less than 4 prior lines. *P* = Fisher's exact test. Note alternative exon usage was defined both using RNA and DNA based approaches with DNA based approaches favoring alternative exon usage. P value determined by Wilcoxon rank sum test.

nature portfolio

Corresponding author(s): Patrick J. Grohar

Last updated by author(s): 3/2/2026

Reporting Summary

Nature Portfolio wishes to improve the reproducibility of the work that we publish. This form provides structure for consistency and transparency in reporting. For further information on Nature Portfolio policies, see our Editorial Policies and the Editorial Policy Checklist.

Statistics

For all statistical analyses, confirm that the following items are present in the figure legend, table legend, main text, or Methods section.

n/a	Confirmed
☐	☒ The exact sample size (*n*) for each experimental group/condition, given as a discrete number and unit of measurement
☐	☒ A statement on whether measurements were taken from distinct samples or whether the same sample was measured repeatedly
☐	☒ The statistical test(s) used AND whether they are one- or two-sided *Only common tests should be described solely by name; describe more complex techniques in the Methods section.*
☐	☒ A description of all covariates tested
☐	☒ A description of any assumptions or corrections, such as tests of normality and adjustment for multiple comparisons
☐	☒ A full description of the statistical parameters including central tendency (e.g. means) or other basic estimates (e.g. regression coefficient) AND variation (e.g. standard deviation) or associated estimates of uncertainty (e.g. confidence intervals)
☐	☒ For null hypothesis testing, the test statistic (e.g. *F*, *t*, *r*) with confidence intervals, effect sizes, degrees of freedom and *P* value noted *Give P values as exact values whenever suitable.*
☒	☐ For Bayesian analysis, information on the choice of priors and Markov chain Monte Carlo settings
☒	☐ For hierarchical and complex designs, identification of the appropriate level for tests and full reporting of outcomes
☒	☐ Estimates of effect sizes (e.g. Cohen's *d*, Pearson's *r*), indicating how they were calculated

Our web collection on statistics for biologists contains articles on many of the points above.

Software and code

Policy information about availability of computer code

Data collection	Clinical data was collected on medidata Rave. No open or custome code was used for genomic data.
Data analysis	Data analysis used standard tools as detailed in methods section.

For manuscripts utilizing custom algorithms or software that are central to the research but not yet described in published literature, software must be made available to editors and reviewers. We strongly encourage code deposition in a community repository (e.g. GitHub). See the Nature Portfolio guidelines for submitting code & software for further information.

Data

Policy information about availability of data

All manuscripts must include a data availability statement. This statement should provide the following information, where applicable:

- Accession codes, unique identifiers, or web links for publicly available datasets
- A description of any restrictions on data availability
- For clinical datasets or third party data, please ensure that the statement adheres to our policy

All genomic data will be deposited into GEO with the accession number GSE322640. Clinical data is compliant with Nature Medicine policy on data sharing policy. All the individual participant data colected during the trial and after de-identification will be shared immediately following publication to researchers who provide a methodologically sound proposal for up to 5 years.

Research involving human participants, their data, or biological material

Policy information about studies with human participants or human data. See also policy information about sex, gender (identity/presentation), and sexual orientation and race, ethnicity and racism.

Reporting on sex and gender	Patients self-reported sex and gender information(24M; 13F). All participants or proxy signed informed written consent. Sex was not part of the design due to the rarity of the disease. No subsequent sex based analysis was performed because sample size is insufficient.
Reporting on race, ethnicity, or other socially relevant groupings	Participant reported race was White (Ph1 89%; Ph2 67%), Asian (Ph1 11%; Ph2 5%), African (Ph2 5%) or ethinicity of Hispanic/Latino (Ph1 11%; Ph2 22%) with the remainder described as not Hispanic/Latino
Population characteristics	The study population had a median age (Ph1 19(10-59); Ph2 21(9-43).
Recruitment	All patients were enrolled in the SARC consortium and selected centers.
Ethics oversight	The study was IRB approved by the central IRB, Western IRB

Note that full information on the approval of the study protocol must also be provided in the manuscript.

Field-specific reporting

Please select the one below that is the best fit for your research. If you are not sure, read the appropriate sections before making your selection.

☒ Life sciences ☐ Behavioural & social sciences ☐ Ecological, evolutionary & environmental sciences

For a reference copy of the document with all sections, see nature.com/documents/nr-reporting-summary-flat.pdf

Life sciences study design

All studies must disclose on these points even when the disclosure is negative.

Sample size	39
Data exclusions	Two patients were excluded in phase I. No data was excluded. Patients were replaced in phase I because they were not evaluable for dose limiting toxicity.
Replication	Replicates (n=3) were used for bulk RNA sequencing. Replicates are not feasible for spatial transcriptomics due to limited tissue but notably contain >3000 data points per sample.
Randomization	This was an open label phase 2 study.
Blinding	This was an open label phase 2 study making blinding not possible.

Reporting for specific materials, systems and methods

We require information from authors about some types of materials, experimental systems and methods used in many studies. Here, indicate whether each material, system or method listed is relevant to your study. If you are not sure if a list item applies to your research, read the appropriate section before selecting a response.

Materials & experimental systems

n/a	Involved in the study
☒	☐ Antibodies
☒	☐ Eukaryotic cell lines
☒	☐ Palaeontology and archaeology
☒	☐ Animals and other organisms
☐	☒ Clinical data
☒	☐ Dual use research of concern
☒	☐ Plants

Methods

n/a	Involved in the study
☒	☐ ChIP-seq
☒	☐ Flow cytometry
☒	☐ MRI-based neuroimaging

Clinical data

Policy information about clinical studies

All manuscripts should comply with the ICMJE guidelines for publication of clinical research and a completed CONSORT checklist must be included with all submissions.

Clinical trial registration	NCT04067115
Study protocol	Targeting the EWS::FLI1 Transcription Factor for Ewing Sarcoma: A Phase 1/2 Study of Trabectedin and Low Dose Irinotecan (SARC037)
Data collection	Clinical data was collected at local sites and reported centrally via Medidata Rave
Outcomes	Primary objectives in Ph1 were: safety, tolerability and recommended Ph2 dose. Secondary objectives were objective tumor response rate (RECIST v1.1), progression free survival, duration of response and 6-month PFS. Primary objective in Ph2 was objective response rate. Secondary objectives were progression free survival, duration of response and 6-month PFS.

Plants

Seed stocks	This article does not report on seed stocks.
Novel plant genotypes	This article does not report on novel plant genotypes.
Authentication	Authentication of plants was not relevant for this study.